Quantifying traffic, biomass burning and secondary source contributions to atmospheric particle number concentrations at urban and suburban sites

J.A. Casquero-Vera, H. Lyamani, G. Titos, M.C. Minguillón, L. Dada, A. Alastuey, X. Querol, T. Petäjä, F.J. Olmo, L. Alados-Arboledas

PII: S0048-9697(21)00348-X

DOI: https://doi.org/10.1016/j.scitotenv.2021.145282

Reference: STOTEN 145282

To appear in: *Science of the Total Environment*

Received date: 11 November 2020

Revised date: 28 December 2020

Accepted date: 15 January 2021

Please cite this article as: J.A. Casquero-Vera, H. Lyamani, G. Titos, et al., Quantifying traffic, biomass burning and secondary source contributions to atmospheric particle number concentrations at urban and suburban sites, *Science of the Total Environment* (2021), https://doi.org/10.1016/j.scitotenv.2021.145282

Quantifying traffic, biomass burning and secondary source contributions to atmospheric particle number concentrations at urban and suburban sites

Casquero-Vera J.A.[1,2], Lyamani H.[1,2], Titos G.[1,2], Minguillón M.C.[3], Dada L.[4], Alastuey A.[3], Querol X.[3], Petäjä T.[4], Olmo F.J.[1,2], Alados-Arboledas L.[1,2]

[1]Andalusian Institute for Earth System Research (IISTA-CEAMA), University of Granada, Autonomous Government of Andalusia, Granada, Spain.
[2]Department of Applied Physics, University of Granada, Granada, Spain
[3]Institute of Environmental Assessment and Water Research (IDAEA), CSIC, Barcelona, Spain
[4]Institute for Atmospheric and Earth System Research (INAR)/Physics, Faculty of Science, University of Helsinki, Helsinki, Finland

Correspondence to: Juan Andrés Casquero Vera (casquero@ugr.es), Andalusian Center for Environmental Research. Autonomous Government of Andalusia-University of Granada, Av. del Mediterráneo s/n. 18006, Granada, Spain.

Abstract.

In this study, we propose a new approach to determine the contributions of primary vehicle exhaust (N_1^{ff}), primary biomass burning (N_1^{bb}) and secondary (N_2) particles to mode segregated particle number concentrations. We used simultaneous measurements of aerosol size distribution in the 12-600 nm size range and black carbon (BC) concentration obtained during winter period at urban and suburban sites influenced by biomass burning (BB) emissions. As expected, larger aerosol number concentrations in the 12-25 and 25-100 nm size ranges are observed at the urban site compared to the suburban site. However, similar concentrations of BC are observed at both sites due to the larger contribution of BB particles to the observed BC at suburban (34%) in comparison to urban site (23%). Due to this influence of BB emissions in our study area, the application of the Rodríguez and Cuevas (2007) method, which was developed for areas mainly influenced by traffic emissions, leads to an overestimation of the primary vehicle exhaust particles concentrations by 18% and 26% in urban and suburban sites, respectively, as compared to our new proposed approach. The results show that (1) N_2 is the main contributor in all size ranges at both sites, (2) N_1^{ff} is the main contributor to primary particles (>70%) in all size ranges at both sites and (3) N_1^{bb} contributes significantly to the primary particles in the 25-100 and 100-600 nm size ranges at the suburban (24% and 28%, respectively) and urban (13% and 20%, respectively) sites. At urban site, the N_1^{ff} contribution shows a slight increase with the increase of total particle concentration, reaching a contribution of up to 65% at high ambient aerosol concentrations. New particle formation events are an important aerosol source during summer noon hours but, on average, these events do not implicate a considerable contribution to urban particles.

Keywords: ultrafine particles, black carbon, biomass burning, road traffic emissions, new particle formation

1 Introduction

Urban and suburban air pollution is a matter of great concern due to its adverse effects on human health and the environment (Murray et al., 2020). Exposure to air pollutants in urban and suburban areas is cause of increased morbidity and mortality, by alterations of the respiratory, cardiovascular and cerebrovascular systems (WHO, 2013). As a result of the implemented abatement policies, emissions of large number of air pollutants decreased in the last decades across Europe (e.g., EEA, 2019), resulting in generally improved air quality across the European Union (EMEP, 2016). Nowadays, most European zones meet the air quality limits established for CO, SO_2 and metals (e.g., Henschel et al., 2013; Querol et al., 2014; EEA, 2019). However, despite these policy efforts during the last decades, in 2017 around 8% and 77% of the EU-28 population was exposed to concentrations of $PM_{2.5}$ (particulate matter with diameter <2.5 μm) exceeding the European air quality standards and the World Health Organization (WHO) Air Quality guidelines, respectively (EEA, 2019).

Particulate matter in urban and suburban environments originates primarily from incomplete fossil fuel combustion, industrial emissions, and products of biomass burning, as well as from non-exhaust vehicle emissions, agricultural emissions, among others (EEA, 2019). Traffic emissions are of particular concern in urban areas and their surroundings, since traffic-related pollutants, particularly aerosol particles, have been associated with overall mortality increase (e.g., Hoek et al., 2000), lung cancer risk (e.g., Beelen et al., 2008) and worsening of respiratory health (e.g., Brauer et al., 2002). The health effects of atmospheric aerosol particles are linked to particle size, as this parameter determines the region of the respiratory system in which the particle would deposit (Gómez-Moreno et al., 2011). However, although several studies have reported that ultrafine particles (UFP; particles with diameters below 0.1μm) are highly associated with morbidity and mortality and respiratory and cardiovascular diseases, no regulations exist concerning the ambient number concentration of UFP (Cassee et al., 2019). In this sense, regulations are based on particle matter (PM) mass concentrations that are mainly controlled by particles in coarse and accumulation mode ranges with negligible influence of UFPs to PM mass concentrations (del Águila et al., 2018). However, UFPs (nucleation and Aitken mode ranges) mainly control ambient particle concentrations in terms of number, with a small contribution of coarser particles to particle number concentrations.

Although UFP exhibit more toxicity than larger particles with the same chemical composition (Johnston et al., 2000; Karlsson et al., 2009), particles' chemical composition also plays an important role in health risks. In this sense, epidemiologic studies have demonstrated the special risks of exposure to carbonaceous aerosols, revealing their strong association with cardiovascular mortality and morbidity (Ito et al., 2011; Ostro et al., 2007). Among carbonaceous aerosols, black carbon (BC) has received increased attention during the past decades. BC is a primary product of incomplete combustion of carbonaceous fuels, mainly originating from diesel engines in urban areas (e.g., Hamilton and Mansfield, 1991; Pakkanen et al., 2000). Besides traffic emissions, biomass burning and domestic heating (based on fossil or biomass fuels) constitute other important sources of BC in Europe. EEA (2019) stimates that for EU-28, 28% and 48% of the anthropogenic BC emissions are from road transport and residential (biomass

and coal) burning sources, respectively. Several studies have shown that improved technologies for new vehicles and increasingly stringent control measures on vehicle emissions have induced a downward trend in ambient BC concentrations during the last decade (e.g., Singh et al., 2018; Lyamani et al., 2011). However, emissions from residential combustion and open-air biomass burning are still not regulated in most European countries, and especially residential wood burning has become a common popular alternative energy source since the last years (Titos et al., 2017). Therefore, there is great interest in identifying and quantifying the contribution of biomass burning to BC concentrations for the development of effective control measures in order to improve air quality in European urban areas.

In addition to primary sources, secondary aerosol has been identified as a significant contributor to fine particulate matter (e.g., Chen et al., 2019). New particle formation (NPF) events are considered an important source of ultrafine secondary aerosol that has been estimated to account for approximately 50% of the total aerosol number concentration in the troposphere (Merikanto et al., 2009). In this sense, urban NPF has been increasingly investigated due to its substantial contribution to the existing primary UFP, together resulting in high particle number concentrations (e.g., Baines et al., 2015; Németh et al., 2018, among others). However, frequency, intensity and duration of NPF events are highly variable, making their contribution to the total particle number concentrations extremely dependent on location and environment where these events occur (Nieminen et al., 2013; Kerminen et al., 2018).

In order to implement effective abatement measures, it is critical to identify the sources of aerosol particles and their contribution to the total aerosol population. Several approaches have been used to quantify the contribution of traffic, biomass burning or secondary sources to the ambient particulate mass concentrations in ambient air. Most of the aerosol source apportionment studies used receptor models, such as Positive Matrix Factorization (PMF) or Chemical Mass Balance (CMB), which use online or offline aerosol chemical composition measurements (e.g., Alves et al., 2011; Minguillón et al., 2015; Tao et al., 2017). On the other hand, Sandradewi et al. (2008) used the spectral aerosol absorption coefficient measurements for quantifying biomass burning and traffic emission contributions to ambient carbonaceous particles with real-time online measurements.

Despite observational studies of source contribution to particle mass concentration have been widely conducted (e.g., Amato et al., 2016; Minguillón et al., 2015), observational studies of the contribution of primary and secondary aerosol particle sources to the total aerosol particle number concentrations are still rather limited (Cai et al., 2020). In the last years, different methods have been proposed to estimate the contribution of particles from primary and secondary sources to ultrafine particle number concentrations (e.g., Beddows et al., 2009, 2015; Cai et al., 2020; Rodriguez and Cuevas, 2007). For instance, Rodríguez and Cuevas (2007) used the relationship between BC and particle number concentration for quantifying the sources and processes contributing to ultrafine particle concentrations in urban ambient air. These authors have devised this method to distinguish between primary and secondary particles in urban areas mainly influenced by traffic emissions, assuming that BC originates only from traffic activities. In this sense, the method of Rodríguez and Cuevas (2007) does not allow to distinguish the sources of primary particles in urban areas where in addition to traffic there are other additional sources of BC. Biomass

burning has been recently recognized as an important source of BC in Europe, even in urban areas (Kalogridis et al., 2018) and hence this source may have a significant contribution to urban aerosol. Therefore, new approach is proposed in this study to separate the contributions of primary vehicle exhaust and primary biomass burning emissions to ambient aerosol in urban areas influenced by biomass burning.

The main objective of this study is the quantification of the contribution of different sources and processes to ultrafine particle concentrations in ambient air at urban and suburban sites influenced by biomass burning emissions. For this, we propose a new approach based on the Rodriguez and Cuevas (2007) and Sandradewi et al. (2008) methods to determine the contribution of both vehicle and biomass burning primary emissions and secondary aerosol to the particle number concentrations. Finally, we apply this new approach to an extended dataset at the urban area in order to investigate the extent of each of the source's contribution to particle number concentrations along the year.

2 Measurement sites and instrumentation

The AMICUS (Aerosol MIcrophysical and Chemical properties at Urban atmoSphere) winter campaign was conducted in the Granada metropolitan area (37.18°N, 3.58°W, 680 m above sea level, a.s.l) from 18-12-2015 to 01-04-2016. The Granada metropolitan area, with a population of approximately 0.53 million inhabitants, is situated in a valley surrounded by mountains of elevation up to 3390 m a.s.l. (Sierra Nevada mountain range). Granada is a non-industrialized medium-sized city where PM_{10} and NO_2 levels frequently exceed the EU threshold limits (Casquero-Vera et al., 2019). Main local aerosol sources affecting the study area are road traffic, domestic heating and biomass burning (Lyamani et al., 2010; Titos et al., 2014). Titos et al. (2017) reported that, during winter, around 40% of the organic matter was from biomass burning origin. In this sense, the AMICUS campaign was designed in order to investigate aerosol sources in urban and suburban environments, with special emphasis on biomass burning and traffic sources impact on Granada metropolitan area. For that, concurrent measurements of aerosol physical and chemical properties were performed using multiple techniques in four monitoring sites situated in the Granada metropolitan area. Two stations were located in historic monuments in order to evaluate the impact of black carbon on monumental heritage (Patrón et al., 2017). Other sampling site, UGR urban station, was located in the urban area of Granada. UGR station is part of AGORA observatory (Andalusian Global ObseRvatory of the Atmosphere) operated in the frame of ACTRIS (Aerosol, Cloud and Trace Gasses Research Infrastructure) (Pandolfi et al., 2018) and also included in the SARGAN (in-Situ AeRosol GAW Network; Laj et al., 2020) and NFAN (NOAA Federated Aerosol Network; Andrews et al., 2019) networks. Considered as representative of urban background conditions, this site was equipped with state-of-the-art in situ and remote sensing instrumentation. Finally, another measurement site was located in the Andalusian Institute of Agricultural and Fisheries Research and Training (IFAPA, "suburban station" from now on) in a rural area ~3 km away from the UGR urban station and ~2 km away from the nearest highway. In order to investigate the impact of the rural activities on the urban area and vice versa, data from both UGR urban and IFAPA suburban measurement sites are considered in this work (see Fig. 1).

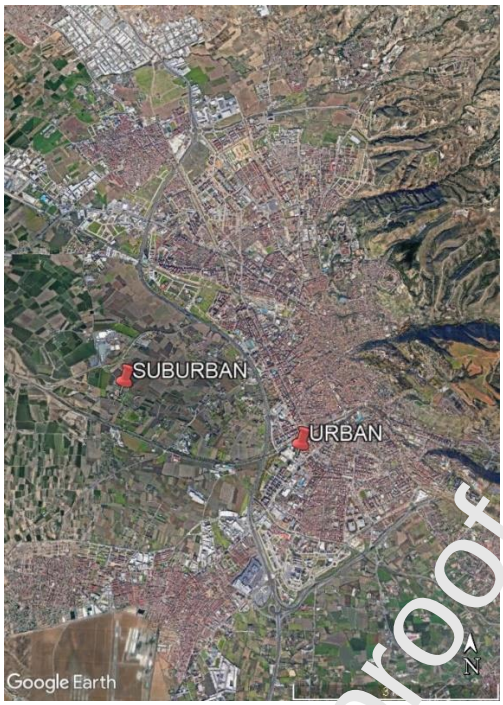

Figure 1. Map showing the location of UGR urban and CAPA suburban stations in Granada metropolitan area

Aerosol chemical and physical properties were monitored at both stations with in-situ techniques. Aerosol properties were measured with same instrumentation model at both measurement sites. Sub-micron aerosol size distribution in the diameter range 12-500 nm were monitored with 5-min temporal resolution by a Scanning Mobility Particle Sizer (SMPS; TSI 3938) composed of an electrostatic classifier (TSI 3082) and a Condensation Particle Counter (CPC; TSI 3772). The quality of the SMPS measurements were checked for flow rates, relative humidity (RH) and 203 nm Poly Styrene Latex particles (PSL) calibration. Following calibration procedures, uncertainty in the measured particle size distribution is within 10% and 20% for the size range 20-200 nm and 200-800 nm, respectively (Wiedensohler et al., 2018). Aethalometer AE33 (Aerosol d.o.o.) was used to obtain 1-min temporal resolution of black carbon mass concentrations, BC, and aerosol light-absorption coefficients at different wavelengths (Drinovec et al., 2015). This instrument is based on filter technique and measure light attenuation (ATN) through a sample-laden filter at seven wavelengths: 370, 470, 520, 590, 660, 880 and 950 nm. Both SMPSs and AE33s systems were intercompared before and after the campaign to ensure the comparability of the data at both stations. In this work, SMPS and aethalometer datasets have been 30-min averaged and only coincident measurements at both sites have been considered in the analyses. In addition, in order to study seasonal variation of particle number concentrations and BC and their sources, 2018 database of SMPS and Aethalometer from UGR urban station are used.

Additionally, during the AMICUS winter campaign an Aerosol Chemical Speciation Monitor (ACSM, Aerodyne Research Inc.) was deployed by IDAEA-CSIC (Institute of Environmental Assessment and Water Research) to measure non-refractory submicron aerosol species (organic aerosols (OA), nitrate, sulfate, ammonium and chloride) in real time (Ng et al., 2011) at UGR urban station. The instrument was

operated with a time resolution of approximately 20 min. Source apportionment of organic aerosol was done in order to estimate biomass burning and hydro-carbon like OA contributions. Further details on the ACSM operation principle and OA source apportionment method can be found in Minguillón et al. (2015).

3 Results

3.1 Sub-micrometric particle number and black carbon mass concentrations

The number size distribution of urban sub-micrometric particles typically exhibits distinct modes which result from different emission sources or chemical and physical processes (e.g., Hama et al., 2017 and references therein). The nucleation mode (particle diameter < 25 nm) consists of primary combustion particles emitted directly into the atmosphere and new particles formed in the atmosphere via gas-to-particle conversion. Aitken mode (25 nm < particle diameter < 100 nm) includes a mixture of soot particles emitted in combustion processes and coagulated nucleation mode particles. Accumulation mode particles (100 nm < particle diameter < 1000 nm) are mainly generated from biomass and fuel combustion processes and coagulation and growth of Aitken mode aerosols by multicomponent condensation of vapors onto the existing particles. Therefore, the analysis of the mode-segregated particle concentrations can provide some information on the sources and processes contributing to particle number concentrations. In this sense, in order to identify the sources and processes contributing to particle number concentration over our sites, we separate the particle number concentrations measured in the range 12-600 nm (N_{Tot}) into three different diameter ranges ($N_{12–25}$ from 12 to 25 nm, $N_{25–100}$ from 25 to 100 nm and $N_{100–600}$ from 100 to 600 nm). In the following sub-sections we analyze the size segregated particle number and BC mass concentrations obtained during the campaign and we also present and discuss the results of the BC source apportionment.

3.1.1 Campaign overview

Table 1 shows the average and standard deviation of particle number concentrations for the different aerosol size ranges obtained at both sites during the whole campaign period. Only concurrent measurements at both sites are considered here. N_{Tot} mean concentration (± standard deviation) at the urban site ($13.4 \pm 9.3 \times 10^3$ cm^{-3}) is slightly higher (13%) than at the suburban site ($11.6 \pm 8.8 \times 10^3$ cm^{-3}). The first streaking pattern here is the very small difference between suburban and urban N_{Tot} levels, the second is that the urban site yields averages close to the typical urban averages for total aerosol number concentration (Cassee et al., 2019). The observed total aerosol number concentrations are similar to those reported (mean value 12×10^3 cm^{-3} during winter 2017) for UGR urban site by Lyamani et al. (2020). These authors also reported that N_{Tot} showed a clear seasonal cycle with higher concentrations during cold season compared to warm season, which they attributed to the increased pollutant emissions from domestic heating and biomass burning as well as the reduced atmospheric boundary layer height and low

atmospheric ventilation in winter (Moreira et al., 2020). The observed concentrations during the AMICUS winter campaign in the urban and suburban sites are slightly higher than those observed in winter season in other Spanish cities like Barcelona, Madrid or A Coruña (Alonso-Blanco et al., 2018). However, the observed concentrations are lower than those observed in other European cities like Leipzig, London, Bern or Glasgow (Putaud et al., 2010). It is worth to note that large part of differences in the aerosol number concentrations among these sites may result from differences in the measured size ranges, measurement height, instrumentation and sampling period.

Table 1. Statistical overview of size-segregated particle number concentrations measured at urban and suburban stations during AMICUS winter campaign. Std is standard deviation.

		N_{Tot} (10^3 cm^{-3})	$N_{12\text{-}100}$ (10^3 cm^{-3})	N_{12-25} (10^3 cm^{-3})	N_{25-100} (10^3 cm^{-3})	$N_{100-600}$ (10^3 cm^{-3})
URBAN	Mean	13.4	10.1	2.1	8.0	3.3
	Std	9.3	7.4	1.8	5.9	2.3
SUBURBAN	Mean	11.6	7.9	1.0	6.9	3.7
	Std	8.8	6.0	1.0	5.5	3.2

When comparing size segregated contributions to the total particle number concentration, particles in the nucleation mode (12-25 nm) have the smallest contribution to the total particle number concentrations, being this contribution slightly larger at the urban site (N_{12-25} represents only 16% and 9% of N_{Tot} at the urban and suburban sites, respectively). In contrast, N_{25-100} represents the largest contribution to N_{Tot} (59% at both sites), being the concentration in this size range slightly larger (by 14%) at the urban site compared to the suburban site. These contributions differ from those reported by Casquero-Vera et al. (2020) for UGR urban station during summertime. These authors used instrumentation with a smaller cut-off size (4 nm) and found that particles in 4-25 nm size range were the main contributor to the total aerosol number concentrations with a contribution of 48%, which is significantly higher than the contribution observed in this study. Casquero-Vera et al. (2020) attributed the high contribution of nucleation mode particles (<25 nm) to the high frequency of regional new particle formation (NPF) events during warm season. Nevertheless, during AMICUS winter campaign, only 3 NPF events occurred. Thus, in addition to the possible discrepancy caused by different cut-off sizes, the low frequency of occurrence of NPF events during the winter campaign may explain the low contribution of nucleation particles to the total number concentration during AMICUS winter campaign as compared to summer. On the other hand, the average contribution of UFP (<100 nm) to the total particle number concentrations is about 75% and 68% at the urban and suburban sites, respectively, which are in the range of those observed by Putaud et al. (2010), who reported 76% as European mean contribution of UFP to the total particle number concentration.

As expected, larger aerosol number concentrations are observed in the 12-25 and 25-100 nm size ranges at the urban site compared to the suburban site (Table 1) due to the proximity of the urban site to traffic

roads. In fact, diurnal patterns of $N_{12–25}$ and N_{25-100} at both sites exhibit distinct morning and evening peaks in coincidence with traffic rush hours, being these peaks much more pronounced in the urban site (Fig. 2 and Fig. S1), which evidence the large impact of traffic emissions, especially at the urban site. In this sense, the large $N_{12–25}$ observed in the urban site could be attributed to larger contribution of the so-called delayed primary particles which are formed in the atmosphere from precursor gases released in hot vehicle exhaust after it dilutes and cools in ambient air (Rönkkö et al., 2017). In addition, the large $N_{25–100}$ observed in urban site could be also related to traffic emissions since carbonaceous particles emitted by EURO standards vehicles contribute to the Aitken mode size fraction (Rodríguez and Cuevas, 2007). In contrast to $N_{12–25}$ and $N_{25–100}$, the mean $N_{100–600}$ concentration at suburban site is 12% larger than that obtained at urban site (Table 1) with less pronounced $N_{100–600}$ morning and evening peaks (Fig. 2). Meanwhile, $N_{100–600}$ concentration represents 32% and 25% of the total particle number concentration at suburban and urban sites, respectively. The additional contribution of other sources different to traffic or aging processes during the aerosol transport to suburban site are probably the reason of the larger $N_{100–600}$ concentration observed at suburban station. Assuming spherical particles and constant particle density for the whole size distribution, particles in accumulation size range (100-600 nm) contribute 92% and 93% to the total mass concentration (12-600 nm) at urban and suburban sites, respectively. Thus, larger particle number concentrations in accumulation mode could imply a significant contribution to particle mass concentrations with important repercussions for air quality. Furthermore, at night time, the total aerosol number concentrations as well as the concentrations of particles in the different ranges in suburban site are quite higher than those observed at the urban site (Fig. 2 and Fig. S1), supporting the presence of important emission sources other than traffic at suburban site. Subsequently, a more detailed analysis of the contribution of different sources to the aerosol number concentrations at both sites will be carried out.

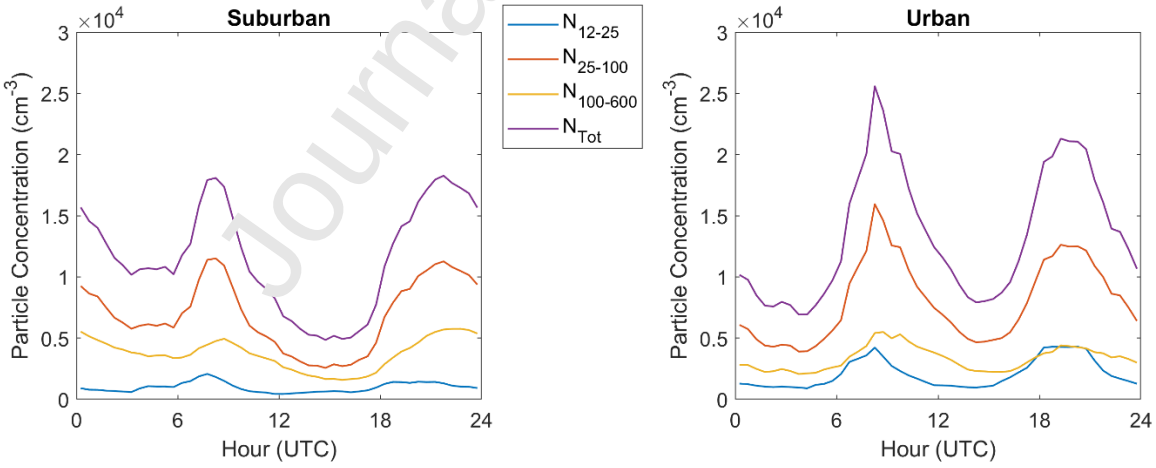

Figure 2. Daily mean pattern of aerosol number concentration in different diameter size rages at suburban and urban sites

Although the suburban site is relatively far from the direct influence of traffic, surprisingly, the concentrations of BC obtained at the urban and suburban sites are similar. In fact, BC concentration ranges from 0.1 to 31 μg m^{-3} with a mean value of 3.0 ± 3.0 μg m^{-3} at the urban site and from 0.1 to 22 μg m^{-3} with a mean value of 2.9 ± 3.0 μg m^{-3} at the suburban site. This result suggests that in addition to

traffic there are other important sources of BC particles at the suburban site. The BC concentrations measured at the urban station are in the range of those found during cold season in other European urban areas. For example, recent studies by Liakakou et al. (2020) in Athens (Greece) and by Costabile et al. (2017) in Rome (Italy) have reported winter mean BC concentrations of 2.8 and 2.9 μg m^{-3}, respectively. However, the BC concentrations obtained at the suburban site are significantly much larger than those reported for suburban sites by Laj et al. (2020) (e.g., SIRTA or Ispra sites).

Figure 3 shows the mean diurnal variation of BC concentrations measured at the urban and suburban sites. As for the total particle number concentration, BC presents a clear diurnal cycle with two distinct peaks associated with traffic emissions at both sites. Furthermore, significantly higher BC concentrations are observed in the suburban site during night hours, which again indicates an additional contribution to BC particles over suburban site from sources other than traffic. Previous observational study in Granada urban area has identified vehicle exhaust and biomass burning as main sources of BC during winter period (Titos et al., 2017). To quantify the contributions of traffic and biomass burning sources to BC concentrations at both sites and confirm whether the night BC increase at the suburban station is due to biomass burning emissions, in the following section we perform the source apportionment analysis of BC particles at both sites.

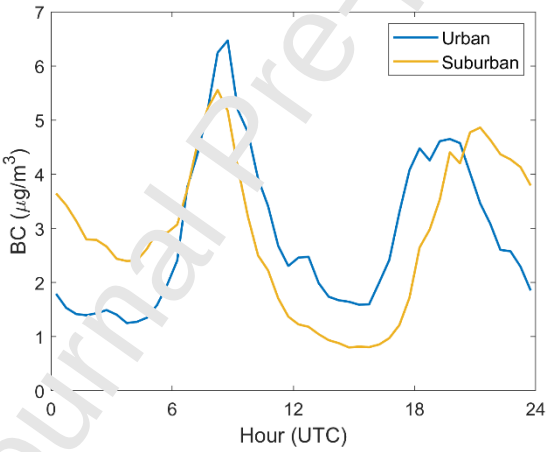

Figure 3. Diurnal mean pattern of BC concentration at the urban and suburban sites

3.1.2 Source apportionment of BC particles

In order to quantify the contribution of vehicle exhaust and biomass burning emissions to ambient BC particles in the urban and suburban sites we used the source apportionment method proposed by Sandradewi et al. (2008). This method assumes that the total aerosol absorption is solely due to the combination of absorption from fossil fuel and biomass burning aerosols. The model is based on the spectral dependency of the absorption coefficient (absorption Angstrom exponent, α) assuming that aerosol absorption from fossil fuel and biomass burning emission sources follows different spectral dependencies and therefore considers the preselection of suitable α values for fossil fuel (α_{ff}) and biomass burning (α_{bb}). Values of α ranging from 0.8 to 1.1 indicate the predominance of BC particles from fuel combustion emissions while α values larger than 1.5 indicate considerable contribution of BC from

biomass burning (e.g., Titos et al., 2017; Helin et al., 2018; Patrón et al., 2017). Several approaches exist to optimize the selection of α_{ff} and α_{bb}, depending on the ancillary measurements available, such as biomass burning tracers from filter samples (e.g., Fuller et al., 2014; Titos et al., 2017) or online chemical speciation measurements (e.g., Ealo et al., 2016). During the AMICUS campaign, an ACSM was operating during a short period at the urban site (from 28 January to 18 February 2016). Thus, following the procedure described by Ealo et al. (2016), optimization of Sandradewi et al. (2008) model was done based on the best correlation between carbonaceous material from fossil fuel (CM_{ff}) and biomass burning (CM_{bb}) with hydro-carbon like organic aerosols (HOA) and biomass burning organic aerosols (BBOA), respectively, obtained from the source apportionment of organic aerosols from the ACSM measurements (Minguillón et al., 2015). Applying this procedure during the period in which the ACSM was operative at UGR urban station, we obtained $\alpha_{ff} = 1.0$ and $\alpha_{bb} = 1.9$. These values of α_{ff} and α_{bb} have been used for BC source apportionment at both measurement sites.

Considering only simultaneous measurements at both sites, the BC, BC_{bb} and BC_{ff} concentrations obtained at the suburban and urban sites during the studied period are shown in Fig 4a. Mean BC_{ff} concentrations of 1.9 ± 2.2 μg m^{-3} and 2.3 ± 2.6 μg m^{-3} are obtained for the whole campaign at the suburban and urban sites, respectively. Thus, the BC_{ff} concentration is only slightly larger at the urban site (1.2 times larger than at suburban site). Furthermore, significantly larger concentrations of BC_{bb} are observed at the suburban site (1.4 times larger than at the urban station), with mean concentrations of 1.0 ± 1.2 μg m^{-3} and 0.7 ± 0.7 μg m^{-3} at the suburban and urban sites, respectively, revealing the strong impact of biomass burning emissions on ambient BC concentrations at the suburban site. Figure 4b shows the diurnal evolution of the relative contribution of biomass burning to total BC concentrations. The contribution of biomass burning along the day is always larger at the suburban site with maximum contribution at both sites (about 40-50%) during night-time (Fig. 4b). The lowest contribution of biomass burning is observed during traffic rush hours at both sites. However, despite the large contribution of traffic to BC concentrations during rush hours, the biomass burning contribution during morning rush hours accounted for the 20% of the total BC concentrations observed at the suburban site and only 10% at the urban station. Overall, biomass burning represents an average contribution of 34% and 23% to the total BC at the suburban and urban sites, respectively, evidencing again the large impact of biomass burning emissions on BC concentrations at the suburban site, especially at night-time (Fig. 4b). Biomass burning contribution to BC concentration at the urban site is in the range of those observed in other European cities. Indeed, a biomass burning contribution of about 25% has been reported for urban and suburban areas in Paris (Favez et al., 2009), 24% in Zurich (Herich et al., 2011) and 23% in London (Fuller et al., 2014). On the other hand, the biomass burning contribution to BC concentration at the suburban station is in the range of those reported for other European metropolitan areas highly influenced by biomass burning like Helsinki (Helin et al., 2018) or those observed in rural areas in Switzerland (Herich et al., 2011), with contributions of 40% and 33%, respectively.

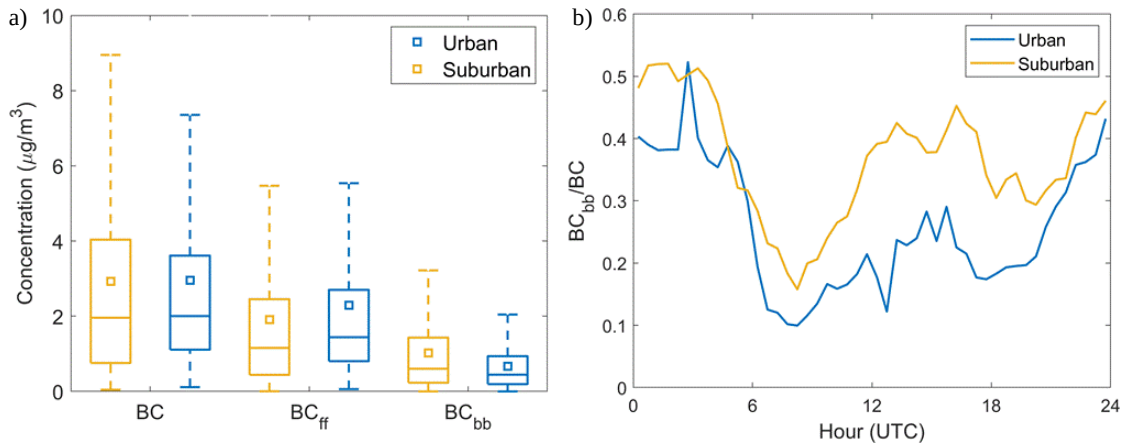

Figure 4. (a) Box and whisker plots of BC, BC_{bb} and BC_{ff} for the suburban and urban sites. The line represents the median of the data, the square represents the mean of the data and the lower and upper edges of the box represent 25th and 75th percentiles of the data, respectively. The length of the whiskers represents 1.5× interquartile range which includes 99.3% of the data. (b) Diurnal evolution of BC_{bb} contribution to BC retrieved for the suburban and urban sites during the study period.

3.2 Contributions of different aerosol sources to total aerosol number concentration

The estimation of the different source contributions to particle number concentration is important for designing efficient measures to reduce air pollution. In order to quantify the sources and processes contributing to the particle number concentrations, Rodriguez and Cuevas (2007) separated total particle number concentrations into two components: primary and secondary particles. Following Rodriguez and Cuevas (2007) criteria, primary component (N_1) comprises particles directly emitted in the particle phase (such as BC, organic matter compounds, polycyclic aromatic hydrocarbons, some trace elements) and particles nucleating immediately after the emissions, so-called delayed primary particles (Rönkkö et al., 2017). On the other hand, secondary component (N_2) includes particles formed by new particle formation (NPF) driven via atmospheric photochemistry or grown by condensation of low-volatility compounds. In this sense, volatile gaseous compounds emitted by traffic are photochemically transformed in the atmosphere to less volatile species, enabling and enhancing secondary aerosol particle formation via condensation or NPF. Whereas the primary particles emissions affect mostly the air quality near the emission source, the effects of the secondary processes are more important on a regional scale (Rönkkö et al., 2017).

To distinguish between particle number concentrations originating from primary emissions and those from secondary processes, Rodriguez and Cuevas (2007) estimated the concentration of primary aerosol particles (N_1) from BC concentrations using the relation:

$$N_1 = S_1 \cdot BC \quad (1)$$

where S_1 is a semi-empirical scaling factor derived from the N_{Tot} vs BC scatter plot (see Fig. S2 of the Supplementary Material), that is interpreted as the minimum number of primary particles arising from vehicle exhaust emissions per each nanogram of BC and is calculated by the quantile linear regression for the 5th percentile.

The results of applying this methodology to all the 30-min averaged data at both stations are shown in Table 2. The obtained value of S_1 is slightly larger (by 14%) at the urban site, meaning that there are 14% more particles per ng of BC at the urban site. This result reveals the large impact of so-called delayed primary particles at the urban station, that could be larger as near as traffic sources are. The obtained S_1 values are in the lower range of the values (2-9 10^6 particles ng(BC)$^{-1}$) reported for other European areas (Rodríguez and Cuevas, 2007; Fernández-Camacho et al., 2010; Reche et al., 2011; Kulmala et al., 2016; Wang et al., 2016; Hama et al., 2017). The lower S_1 values obtained in this study could be related with the implementation of more stringent EURO emissions standards along the last years. In this sense, Euro VI standards (implemented in 2015) are 5 times stricter than Euro IV (implemented in 2006), reducing the limit of particles matter emissions from 25 mg/km (98/69/EC) to 5 mg/km (715/2007/EC). In addition to the stringent measure to reduce particles matter emissions in the last decade, control of particle number concentration emissions started since EURO V implementation limiting the emissions to 6×10^{11} part/km (692/2008/EC) to all car registrations since 2013. Nevertheless, part of the differences in S_1 values reported in the literature could be also related to the influence of different ambient air conditions on new particle formation during dilution and cooling of vehicle exhausts. Also, it is worth to mention that the comparison among studies depends on the instrumentation used and it is especially sensitive to the CPC cut-off size or SMPS diameter range.

Table 2. Mean particle number concentration and contribution to total particle concentrations in parentheses as well as scaling factors obtained by the different approaches used. N_1 and S_1 are the concentration of primary particles and scaling factor obtained by Rodriguez and Cuevas (2007) while N_1^{ff}, N_1^{bb} and N_2 are the concentrations of primary vehicle exhaust, primary biomass burning and secondary particles, respectively, and S_1^{ff} is scaling factor determined by the proposed method.

	Particle number concentration (10^3 cm^{-3})				**Scaling factors (10^6 particles ng(BC)$^{-1}$)**	
	N_1	N_1^{ff}	N_1^{bb}	N_2	S_1	S_1^{ff}
URBAN	6.67 (50%)	5.44 (41%)	1.23 (9%)	6.73 (50%)	2.20	2.38
SUBURBAN	6.04 (52%)	4.49 (39%)	1.55 (13%)	5.56 (48%)	1.93	2.29

Although the minimum particles emitted per ng of BC (S_1) in this study is below those reported in other areas, the contribution of primary particles to the total particle number concentration (50% and 52% at urban and suburban sites, respectively) was slightly larger than the contribution observed in other cities like Barcelona (46%), Santa Cruz de Tenerife (46%) or Leicester (43%) (Reche et al., 2011).

At this point, it is important to recall that the Rodriguez and Cuevas (2007) method, as was devised, assumes that BC particles are only originated from traffic emissions. However, this assumption is not valid in areas influenced by biomass burning emissions, where the application of this methodology can lead to significant overestimation of the primary particles associated to vehicle emissions. Therefore, new approach is proposed in this study to separate the contributions of primary vehicle exhaust and primary biomass burning emissions to ambient aerosol in urban areas influenced by biomass burning. To this end we propose the use of BC originated only from traffic emissions, BC_{ff}, previously estimated with the Aethalometer model:

$$N_1^{ff} = S_1^{ff} \cdot BC_{ff} \quad (2)$$

where S_1^{ff} is a scaling factor derived from the N_{Tot} vs BC_{ff} scatter plot and N_1^{ff} is the concentration of primary particles from traffic exhaust (see Fig. S2 of the Supplementary Material). The results of applying this methodology to all the 30-min averaged data at both stations are shown in Table 2. The estimated N_1^{ff} mean concentration is of 5.44 × 10^3 cm^{-3} and 4.49 × 10^3 cm^{-3} at the urban and suburban sites, respectively, showing that the application of Rodriguez and Cuevas (2007) method in the study area lead to the overestimation of the concentration of primary particles emitted from vehicle exhaust by about 18% and 26% at urban and suburban sites, respectively (Table 2). Thus, this proposed method lead to a reduced contribution of primary emission of vehicle exhaust to the total aerosol number concentration during the whole campaign, decreasing from 50% and 52% at urban and suburban stations, respectively, estimated by the Rodriguez and Cuevas (2007) method, to 41% and 39% at the urban and suburban sites, respectively, estimated by the proposed method.

Considering the main aerosol emission sources on the study region, we can assume that the only significant combustion process contributing to BC concentrations at urban and suburban environments are traffic exhaust and biomass burning. Thus, the concentration of primary particles from biomass burning (N_1^{bb}) can be estimated as:

$$N_1^{bb} = N_1 - N_1^{ff} \quad (3)$$

and, following Rodriguez and Cuevas (2007) definition, the concentration of secondary particles (N_2) could be estimated as:

$$N_2 = N_{Tot} - N_1^{ff} - N_1^{bb} \quad (4)$$

A statistical summary of the particle number concentrations of primary particles from biomass burning and secondary particles are reported in Table 2. The results show that primary biomass burning particles with concentrations of 1.23 × 10^3 cm^{-3} and 1.55 × 10^3 cm^{-3} contributed 18% and 26% to the total primary particles at the urban and suburban sites, respectively. These N_1^{bb} concentrations represent 9% and 13% of the total particle concentrations at the urban and suburban sites, respectively, revealing that the contributions of primary biomass burning source to particle number concentration cannot be neglected. Finally, with concentrations of 6.73 × 10^3 cm^{-3} and 5.56 × 10^3 cm^{-3} at the urban and suburban sites,

secondary source contribution to total particle number concentrations (50% at the urban site and 48% at the suburban site) is comparable to the contribution of both primary sources.

Although primary and secondary sources show similar relative contributions to the total aerosol number concentrations at both sites, Figure 5 shows that these contributions vary with the total particle number concentration. Figure 5 shows that secondary aerosol is the main contributor to the total particle number concentrations at low concentrations at both sites, especially at urban site. However, at urban site, the contribution of traffic source shows a slight increase with the increase of N_{Tot}, reaching a contribution of up to 65% at high ambient total particle number concentrations. Thus, a reduction in exhaust traffic emissions will help to reduce substantially high total particle concentrations at urban site. On the other hand, biomass burning source is the smaller contributor to total particle number concentrations at both sites with no clear variation of this source contribution with the variation of the total particle concentration.

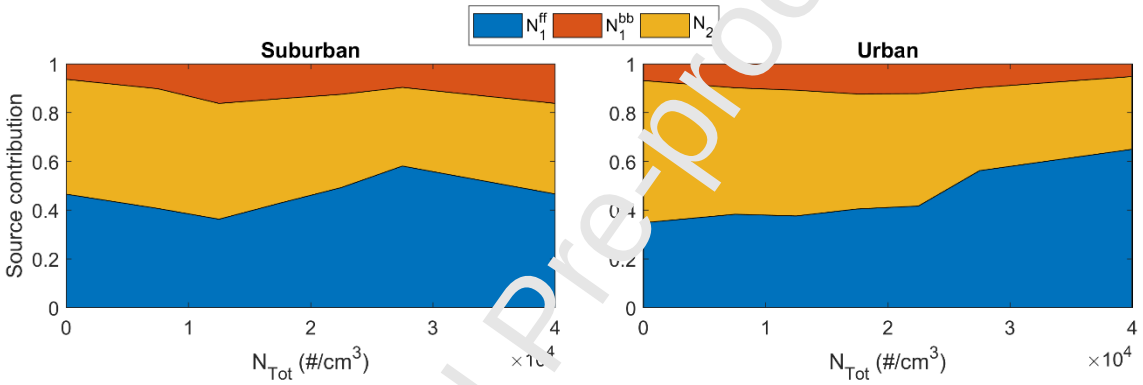

Figure 5. Contributions of primary traffic and biomass burning as well as secondary particles to total particle number concentrations as function of total particle number concentration.

3.3 Mode-segregated particle sources contribution

As mentioned above, knowledge of the contribution of primary and secondary sources to the total particle number concentration gives valuable information for improving current abatement strategies. However, understanding the contribution of these sources as a function of particle size could provide definite evidence to help tackling high air pollution levels and providing valuable information in terms of health effects. As was done by Kulmala et al. (2016), we extended the analysis presented in the previous section to the three aerosol size ranges (12-25, 25-100 and 100-600 nm), which will allow us not only to split the total particle number concentrations into N_1^{ff}, N_1^{bb}, N_1 and N_2, but also to split it for each single size range. Thus, using the new methodology presented in section 3.2 and following the mentioned criteria, the total particle number concentration in nucleation size range (12-25 nm) is split into four components: N_{11} (total primary particles), N_{11}^{ff} (primary vehicle exhaust particles), N_{11}^{bb} (primary biomass burning particles) and N_{21} (secondary particles). Similarly, particle number concentration for the other

size ranges is split into N_{12}, N_{12}^{ff}, N_{12}^{bb} and N_{22} for 25-100 nm size range and N_{13}, N_{13}^{ff}, N_{13}^{bb} and N_{23} for 100-600 nm size range.

A statistical summary of the particle number concentrations of the four components (total primary particles, primary particles from biomass burning and vehicle exhaust and secondary particles) for the three size ranges (12-25, 25-100 and 100-600 nm) and scaling factors are reported in Table 3. Strong to moderate correlations (r>0.70) between particle number concentrations in 25-100 and 100-600 nm size ranges and BC concentration are observed at both sites (not shown). However, the nucleation mode particle concentration (12-25 nm size range) has relatively weak correlations with BC at the suburban and urban sites (correlation coefficient of 0.44 and 0.67, respectively). This is because a large fraction of nucleation mode particles is probably not associated with fresh traffic emissions, especially at suburban site. Thus, the results of source contributions to nucleation mode aerosol should be interpreted with caution.

Table 3. Mode segregated particle number concentrations from primary vehicle exhaust, primary biomass burning and secondary origin and scaling factors at urban and suburban sites. N_{11}, N_{11}^{ff}, N_{11}^{bb} and N_{21} are the concentrations of total primary, primary vehicle exhaust, primary biomass burning and secondary particles in the 12-25 nm size range, respectively. N_{12}, N_{12}^{ff}, N_{12}^{bb} and N_{22} and N_{13}, N_{13}^{ff}, N_{13}^{bb} and N_{23} are the corresponding concentrations in 25-100 nm and 100-600 nm size ranges, respectively. The contribution of each source to total particle concentration in each size mode is given in parentheses.

	Particle number concentration (10^3 cm^{-3})											
	N_{11}^{ff}	N_{11}^{bb}	N_{11}	N_{21}	N_{12}^{ff}	N_{12}^{bb}	N_{12}	N_{22}	N_{13}^{ff}	N_{13}^{bb}	N_{13}	N_{23}
URBAN	0.59 (28%)	0.05 (2%)	0.64 (30%)	1.46 (70%)	3.52 (44%)	0.51 (6%)	4.03 (50%)	3.97 (50%)	1.20 (36%)	0.30 (9%)	1.50 (45%)	1.80 (55%)
SUBURBAN	0.18 (18%)	0.00 (0%)	0.18 (18%)	0.82 (82%)	2.67 (39%)	0.86 (12%)	3.53 (51%)	3.37 (49%)	1.07 (29%)	0.41 (11%)	1.48 (40%)	2.22 (60%)

	Scaling factors (10^6 particles ng(BC)$^{-1}$)					
	S_{11}^{ff}	S_{11}	S_{12}^{ff}	S_{12}	S_{13}^{ff}	S_{13}
URBAN	0.26	0.22	1.54	1.37	0.53	0.51
SUBURBAN	0.09	0.05	1.37	1.18	0.55	0.50

The results of applying the methodology presented in this study to size-segregated particle number concentrations evidences a distinct contribution of primary and secondary sources to each size mode. As shown in previous section, secondary aerosol is the main contributor to total particle number concentrations at the urban and suburban sites, followed by primary particles from vehicle emissions and primary biomass burning particles. Looking at size-segregated contributions, secondary aerosol is also the main contributor in the 12-25 and 100-600 nm size ranges at the urban and suburban sites. In this sense, secondary aerosol represents 70% and 82% of the particles in the 12-25 nm size range and 55% and 60% in the 100-600 nm size range, at the urban and suburban sites, respectively. However, the contribution of primary particles (from both vehicle exhaust and biomass burning) is similar to that of secondary particles in the 25-100 nm size range, where the primary particles represent 50% and 51% of the particle number concentration at the urban and suburban sites, respectively. When looking at primary particles, vehicle exhaust is the main contributor to primary particles accounting for more than 70% of the total primary particles in all the studied size ranges. These results are in agreement with the source apportionment of BC, where BC_{ff} originated from traffic emissions accounted for 66% and 77% of the total BC at suburban and urban sites, respectively.

When comparing particle number concentration at the urban and suburban sites, primary vehicle exhaust and total primary particles concentrations are larger at the urban site in all the size ranges. However, secondary aerosol presents larger concentrations at suburban site in the 100-600 nm size range, with concentrations of 2.20×10^3 and 1.80×10^3 cm^{-3} at the suburban and urban sites, respectively. In addition, the concentration of primary biomass burning particles at suburban site is 1.7 and 1.4 times larger than at urban site in the 25-100 and 100-600 nm size ranges, respectively. In this sense, the concentration of primary biomass burning particles represents 24% and 13% of the total primary particle number concentrations in the 25-100 nm size range and 28% and 20% in the 100-600 nm size range at the suburban and urban sites, respectively. Thus, considering that the particles in the 100-600 nm size range represents more than 90% of the total mass concentration, this significant contribution of biomass burning particles especially in the 100-600 nm size range would imply a significant contribution of this source to particle mass concentration with important repercussions for air quality.

Diurnal patters of the mode segregated particle number concentrations of primary and secondary particles at the urban and suburban sites are shown in Fig. 6. The primary vehicle exhaust particle concentration in the different size ranges considered exhibits a marked morning and evening peaks in coincidence with traffic rush hours. This pattern is observed at both suburban and urban sites, however, a peak delay is observed between both sites as it was observed for BC on section 3.1. In this sense, the morning peak on vehicle primary exhaust particle concentration at suburban site is observed prior to that at urban site and during the evening hours the suburban peak is delayed few hours respect to the observed on urban site. This delay can be explained by the variation of the wind diurnal pattern observed in the study area and the location of the main sources of particles. The urban site is ~3 km away from suburban site and between both stations is located the main highway that surrounds the city (400 m away from urban site). In this sense, the study region has a characteristic mountain-valley wind regime, with up-valley winds from NW-W during day time and down-valley winds from SE-E during night (Lyamani et al., 2020; Ortiz-

Amezcua, 2019) that could explain the dissimilarities observed in diurnal patterns of the primary vehicle exhaust particle concentration at the suburban and urban sites.

Diurnal evolution of primary biomass burning particles concentrations in the 25-100 and 100-600 nm size ranges show higher values during the evening-night hours at both measurement sites. However, the increase of biomass burning primary particles is especially marked at the suburban site, where the total particle concentration and the concentration in the 25-100 and 100-600 nm size ranges are 7 times larger during night-time than during day-time. In this sense, during night-time, up to 45% and 39% of the total primary number concentrations at the suburban and urban sites, respectively, resulted from biomass burning source. In terms of absolute concentrations, higher concentration of primary biomass burning particles is observed at suburban site with mean concentration of 1.6×10^3 cm^{-3} (1.2×10^3 cm^{-3} at urban site).

The size segregated concentrations of secondary particles at suburban site do not show clear daily pattern during the study period. However, at urban site the concentration of secondary particles shows two marked peaks in all the size ranges, except in 100-600 nm size range, in coincidence with traffic rush hours. At urban site, the secondary particles in 12-25 nm size range is the main contributor along the whole day. In this sense, the lower temperatures during winter season may be more favorable for secondary particle formation through particle condensation and nucleation during cooling and dilution of vehicle exhaust (Rönkkö et al., 2017). Also, the increase on N_2, especially during evening- and night-time, could be a consequence of the contribution of secondary organic aerosol formation from biomass burning emissions.

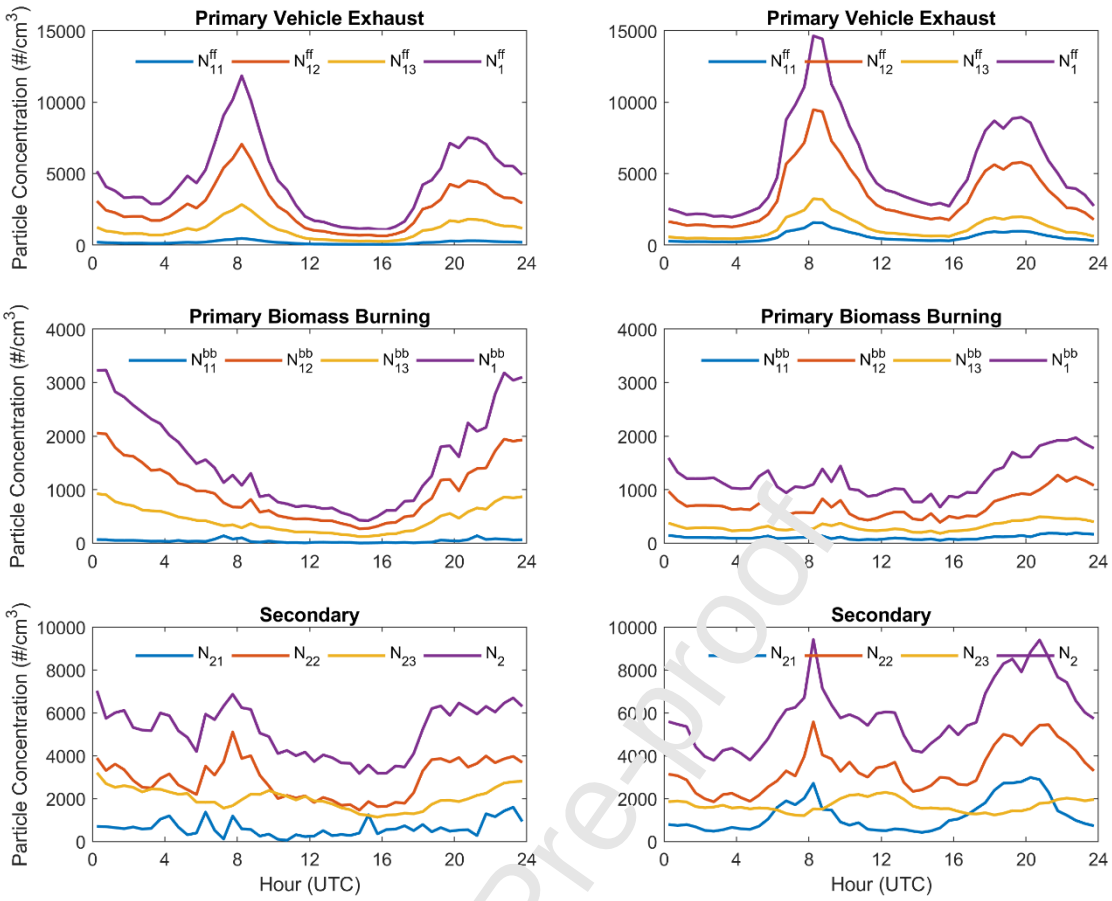

Figure 6. Diurnal evolution of mode segregated and total particle number concentrations from primary vehicle exhaust, primary biomass burning and secondary origin at suburban (left column) and urban sites (right column). N_{11}, N_{11}^{ff}, N_{11}^{bb} and N_{21} are the concentrations of total primary, primary vehicle exhaust, primary biomass burning and secondary particles in the 12-25 nm size range, respectively. N_{12}, N_{12}^{ff}, N_{12}^{bb} and N_{22} and N_{13}, N_{13}^{ff}, N_{13}^{bb} and N_{23} are the corresponding concentrations in 25-100 nm and 100-600 nm size ranges, respectively.

3.4 Seasonal variability of aerosol number concentrations originating from different primary and secondary sources

The variability of aerosol number concentration in urban environments is largely determined by local emission sources and atmospheric processes. Particle emission sources has been widely recognized to present seasonal variability. In Granada metropolitan area, domestic heating (based on fuel oil combustion and biomass burning) and agricultural wastes burning for land clearing represent an additional local source of aerosols in winter (Titos et al., 2017). In opposite, traffic activity in Granada city remains almost constant along the year, with only a slight decrease during summer due to holidays period. On the other hand, the occurrence of new particle formation events at Granada shows a marked seasonal variability, with high occurrence frequency in spring and summer (as can be seen below). So, to investigate the impact of these different aerosol sources and their contributions to the total aerosol number

concentrations throughout the year, in this section we apply the newly proposed methodology to aerosol number and BC concentrations measured during 2018 in the UGR urban station. As until now there is no reference source apportionment method that can be used to quantitatively evaluate the performance of the new method proposed, the following seasonal analysis may help to qualitatively address its feasibility as well as to investigate the temporal variability of primary and secondary sources in the Granada urban area.

A statistical summary of aerosol number concentrations of primary vehicles exhaust, primary biomass burning and secondary particles as well as scaling factors obtained at UGR urban station for each season is displayed in Table 4. In this section, winter corresponds to the months from December to February, spring from March to May, summer from June to August and autumn from September to November.

Table 4. Seasonal statistical summary of particle number concentration and the corresponding contribution of the different sources to total particle concentrations (in parentheses) as well as scaling factors obtained at UGR station for 2018. N_1 and S_1 are the concentration of total primary particles and scaling factor obtained by Rodriguez and Cuevas (2007) while N_1^{ff}, N_1^{bb} and N_2 and S_1^{ff} are the concentrations and scaling factor determined by the proposed method.

	Particle number concentration (10^3 cm^{-3})				Scaling factors (10^6 particles ng(BC)$^{-1}$)	
	N_1	N_1^{ff}	N_1^{bb}	N_2	S_1	S_1^{ff}
Winter	7.27 (48%)	5.66 (37%)	1.61 (11%)	7.90 (52%)	2.50	2.72
Spring	4.40 (45%)	3.91 (40%)	0.49 (5%)	5.44 (55%)	3.30	3.30
Summer	4.62 (51%)	4.27 (47%)	0.35 (4%)	4.41 (49%)	3.16	3.15
Autumn	5.78 (48%)	5.32 (43%)	0.46 (5%)	6.35 (52%)	2.60	2.78

In all seasons, total particle number and BC concentrations shows strong to moderate correlations ($r>0.66$). The estimated S_1^{ff} slope shows an evident seasonal variation with the highest slope values during warm seasons and lowest during cold season (Table 4). This seasonal behaviour is probably associated with a smaller reduction of particulate emission rates in comparison with the reduction of BC emission rates from cold to warm period due to the seasonal change in meteorological conditions (e.g., relative humidity and temperature). In this sense, it is well known that both aerosol particles and especially BC emissions from fuel combustion increase with decreasing temperature (e.g., Olivares et al., 2007; Chan et al., 2014).

Total particle number concentration at UGR urban station shows a clear seasonal pattern. Largest and smallest total particle number concentrations are observed during winter (1.51×10^4 cm^{-3}) and summer (0.90×10^4 cm^{-3}), respectively (N_1+N_2 on Table 4). Similar seasonal variations in aerosol number concentrations were reported for other urban areas (e.g. Järvi et al., 2009; Ripamonti et al., 2013). This

seasonal variation is attributed to the increased emissions from domestic heating, burning of residual agricultural waste in the agricultural area surrounding the site (Titos et al., 2017; Lyamani et al., 2020). Furthermore, the reduced mixing volume and low wind speed observed in the study area during cold period (Lyamani et al., 2020; Moreira et al., 2020) would favour lower vertical and horizontal dilution of the aerosol emissions, contributing to the increase in aerosol concentration in winter months.

As can be seen in Table 4 and as expected, vehicle exhaust is the main source of primary particles along the year in UGR urban station with mean concentrations ranging from 5.66×10^3 cm^{-3} in winter to 3.91×10^3 cm^{-3} during spring season. Since traffic activity remains almost constant along the year in Granada city, this difference on vehicle exhaust primary particles could not be due to larger traffic activity during winter period. Thus, the increase of vehicle exhaust primary particles could be due to lower atmospheric boundary layer heights and lower ambient temperatures. In this sense, ambient temperatures could influence the vehicle particle emissions, with emissions increasing at colder temperatures and during cold start conditions that lead to inefficient combustion, inefficient catalyst operation and the potential for the vehicle operation under fuel-rich conditions (Nam et al., 2010).

Despite the concentration of vehicle exhaust primary particles peaks in winter, it coincides with the lowest contribution of traffic primary particles to total primary particles due to the highest biomass burning primary particle concentrations observed during winter period with concentrations of 1.61×10^3 cm^{-3}, that represents 22% of the total primary particles concentration. For the other seasons, as expected, the absolute concentration as well as the contribution of biomass burning source to the measured aerosol number concentrations are negligible (below 8%).In this sense, agricultural waste and biomass burning from domestic heating practices are common in the study area during the cold season, and especially domestic heating based on olive pits burning has significantly increased over the past years (Titos et al., 2017). However, these sources are negligible during warm season due to the prohibition of open-air biomass burning activities during that period and the absence of domestic heating.

As it was previously observed in other urban areas, secondary particles presented an important contribution to total aerosol number concentration at UGR urban station through the year with contributions ranging from 40% to 55. The high winter concentration (7.90×10^3 cm^{-3}) and contribution (52%) of secondary particles is, in large part, associated with the lower temperatures during this cold season which favour more secondary particle formation during cooling and dilution of vehicle exhaust through nucleation and condensation processes of emitted condensable gaseous compounds. Summarising, in winter the secondary particles are the main contributor to total number concentration (52%) at UGR urban station followed by primary exhaust particles (37%) and biomass burning particles (11%) while in summer season the secondary particles and primary exhaust particles contribute 49% and 47% to the total aerosol number concentration, respectively.

Analysis of seasonal diurnal variability can give us more insights about the seasonal change in source emission rates and processes affecting aerosol load. Figure 7 shows the seasonal diurnal evolutions of the particle number concentrations from each primary source and secondary origin at urban site. As expected, in all season, the concentration of traffic primary particles shows a clear diurnal pattern with two marked

peaks in coincidence with traffic rush hours, being primary particles from vehicle exhaust the main contributor to the total number concentration during the morning traffic rush hours. The diurnal evolution of secondary particle concentrations during autumn and winter shows similar evolution to traffic diurnal pattern with two peaks in coincidence with traffic rush hours. However, the evening peak at both seasons shows longer duration, ending much later than the primary vehicle exhaust peak. In addition, the evening peak of secondary particle concentration is much pronounced than the morning one, especially in winter season, being secondary particles the most important contributor to the total number concentration during evening and night-time. This diurnal behavior is different to the showed by the concentration of primary vehicle exhaust particles, which showed higher concentration during the morning peak than during evening peak in all season. Thus, this result points to an important contribution of domestic heating emissions to secondary aerosol number concentration at evening-night hours during cold period.

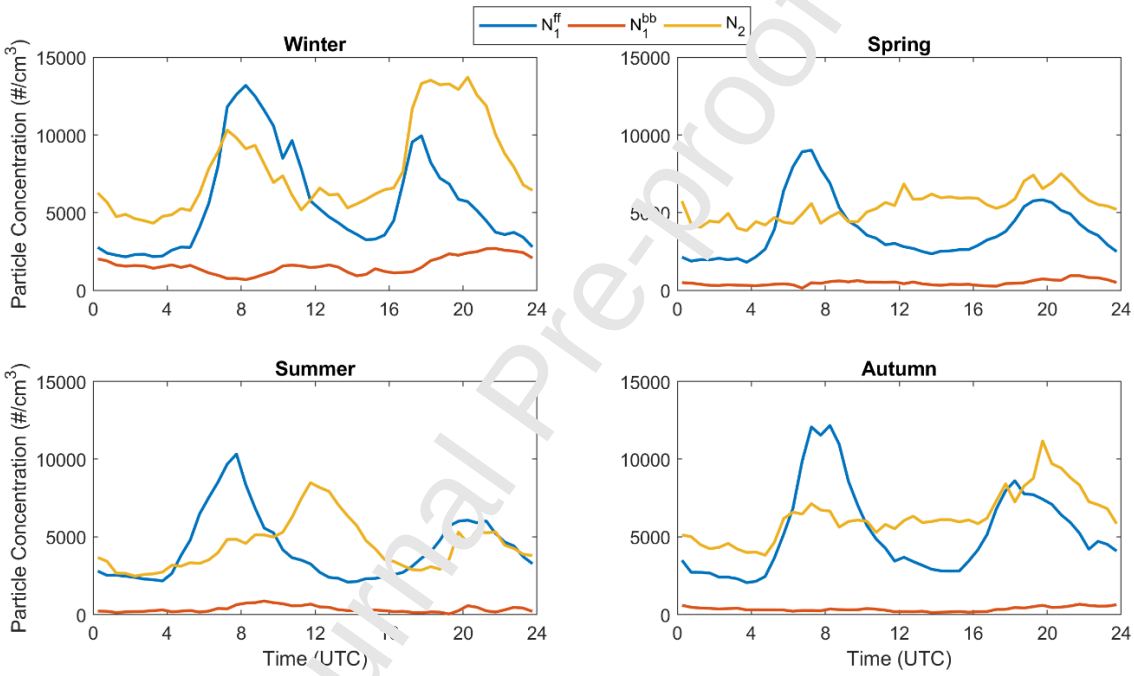

Figure 7. Seasonal diurnal evolution of total particle number concentration from primary (fossil fuel and biomass burning) and secondary origin at urban site.

On the other hand, the secondary particle concentration in summer shows a pronounced increase at noon four hours after the morning peak of primary traffic particles, indicating that is not directly related to vehicle emissions. Also, this pronounced noon peak is not observed in the rest of seasons. This noon peak in concentration of secondary particles is attributed to the high occurrence frequency of regional NPF events during warm period, as discussed below.

In order to determine the significance and relative contribution of atmospheric NPF events to particle number concentrations, we analyzed the NPF events that occurred during 2018. Following Dal Maso et al. (2005) procedure, days has been classified as event, non-events, undefined and bad-data days. The results show 99 days of NPF events, 132 non-event and 33 undefined days for a total of 264 analyzed days, with an event frequency of 38% for 2018 year. However, despite the event frequency is in the range

of those observed in other southern area of Spain (Sorribas et al., 2015) or Finnish boreal forest (Dal Maso et al., 2005), the monthly variability of NPF events frequency is significantly larger than that observed in those studies. Figure 8 shows that the occurrence of NPF events in the study region have a large variability along the year, with an event frequency ranging from 4% on December to 100% on July. In this sense, NPF events occurs mainly during the warm season, later spring and early autumn.

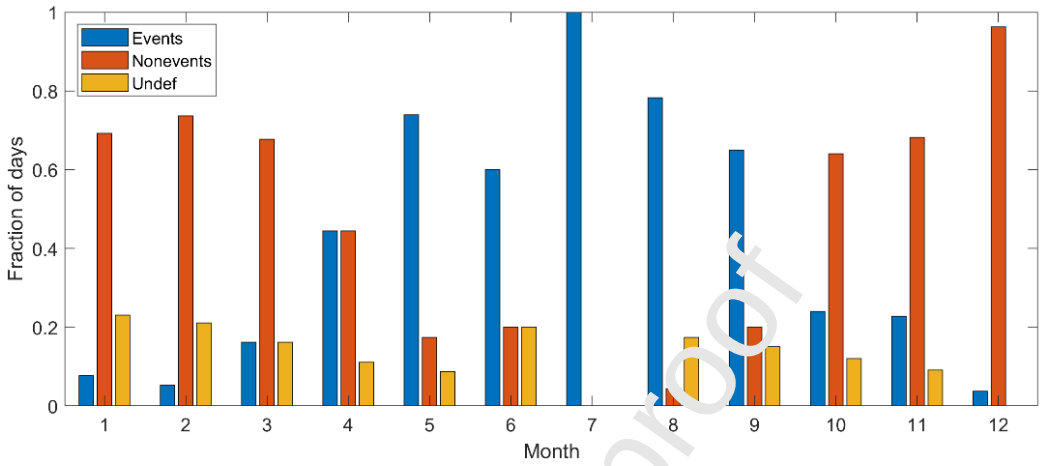

Figure 8. Monthly fraction of days classified as NPF events, nonevents and undefined.

In order to study the relative concentration increment of particles from NPF with respect to the particles originating from all other sources on event days, we applied Salma et al. (2014) methodology for 2018 NPF events. Salma et al. (2014) defined the nucleation strength factor (NSF) as the particle number concentration ratio of ultrafine particles to the regional aerosol in accumulation mode on NPF days to non-NPF days, respectively:

$$NSF = \frac{(N_{12-100}/N_{100-600})_{events}}{(N_{12-100}/N_{100-600})_{non-events}} \quad (5)$$

The importance of atmospheric NPF is negligible if NSF<1.0. In case of 1.0<NSF<2.0, NPF shows comparable importance to all other sources. When NSF>2.0, the NPF has the highest contribution to ambient particles than any other sources.

Mean nucleation strength factor of 1.05 has been obtained in Granada urban site during 2018. This implies that, on average, regional new particle formation does not implicate a considerable contribution of NPF events to total urban particles. This value is significantly lower than those observed in central European cities Budapest, Vienna, and Prague, with NSF values of 1.58, 1.54, and 2.01, respectively (Németh et al., 2018). Large part of these differences in NSF factor is attributed to the differences in cut-off sizes of the used instruments. On the other hand, the summer diurnal pattern of NSF shows that the nucleation strength factor varies from ~0.7 during early morning to ~2 at noon (not shown). Thus, in summer, NPF events is an important source of particles during hours of high solar radiation, however, traffic primary particles and secondary particles from other sources different to NPF events are the main sources of particles in the urban area of Granada.

4 Conclusions

In order to implement effective abatement measures, it is critical to identify the sources of aerosol particles and their contributions to the total aerosol population. For this purpose, we proposed a new approach based on Rodriguez and Cuevas (2007) and Sandradewi et al. (2008) methods to determine the contributions of both vehicle exhaust and biomass burning primary as well as secondary particles to total and mode segregated particle number concentrations. For that, we used simultaneous measurements of aerosol size distribution in 12-600 nm size range and black carbon (BC) concentration performed at urban and suburban sites in Granada, Spain, during AMICUS winter campaign in 2015-2016.

As expected, larger aerosol number concentrations, especially in the 12-25 and 25-100 nm size ranges, are observed at the urban site compared to the suburban site. Surprisingly, similar concentrations of BC are observed at both sites due to the larger contribution of biomass burning particles to the observed BC at suburban (34%) in comparison to urban site (23%). Due to the significant biomass burning contribution, it has been found that in the study areas the application of Rodriguez and Cuevas (2007) method, which only assume primary particles from vehicle exhaust, leads to the overestimation of the concentration of primary particles emitted from vehicle exhaust by about 18% and 26% at urban and suburban sites, respectively.

The results of the new proposed approach show that at both sites secondary particles are the main contributor to mode segregated particle number concentrations, especially in the 12-25 and 100-600 nm size ranges, followed by primary particles from vehicle emissions and primary biomass burning particles, respectively. In both sites, primary particles from vehicle exhaust dominated the total primary particles (>70%) at all the studied size ranges. The concentration of primary biomass burning particles in the 25-100 nm and 100-600 nm size ranges at suburban site is 1.7 and 1.4 times larger than at urban site, respectively, being the contribution of primary biomass burning particles to the total primary particle number concentrations 24% and 13% in the 25-100 nm size range and 28% and 20% in the 100-600 nm size range at the suburban and urban sites, respectively. The different source contributions vary with the total particle number concentration, being secondary particles the main contributor at low particle number concentrations at both sites. At urban site, the contribution of primary particles from traffic emissions shows a slight increase with the increase of total particle number concentration, reaching a contribution of up to 65% at high ambient particle number concentrations. Thus, these results could give valuable information on the qualitative effect of various types of abatement measures.

Finally, we applied this new approach to an extended dataset at the urban site in order to examine sources' strength along the year and their contributions to particle number concentrations. As expected, vehicle exhaust is the main source of primary particles along the year in UGR urban station. The concentrations of primary particles from biomass burning source was highest in winter (1.6×10^4 cm^{-3}), when this source contributed about 22% to the total concentration of primary particles. New Particle Formation process (NPF) has been found to be an important source of particles only during summer noon

hours but, on average, NPF events does not implicate a considerable contribution to atmospheric particles in the urban environment.

The proposed new approach has been shown to be a useful tool for assessing and quantifying sources contributing to particle number concentrations into different aerosol size ranges under the influence of vehicle exhaust and biomass burning emissions. Thus, considering the instrumentation used, this new approach could be useful in assessing the impact of these sources around the globe since this methodology can be applied to larger datasets (as those generated by ACTRIS or SARGAN networks), giving more insights into secondary and primary contributions (vehicle exhaust and biomass burning) and into the health effects of these aerosol sources.

5 Acknowledgments

Juan Andrés Casquero-Vera is funded by MINECO under the predoctoral programme FPI (BES-2017-080015). Gloria Titos is funded by Spanish Ministry of Science and Innovation under postdoctoral program Juan de la Cierva (IJCI-2016-29838). This work was supported by the Spanish Ministry of Economy and Competitiveness through projects CGL2016-81092-R, CGL2017-90884-REDT and RTI2018.101154.A.I00, by the Andalusia Regional Government, University of Granada and FEDER funds through projects B-RNM-496-UGR18 and P18-RT-3820, and by the University of Granada through Plan Propio Programs: Visiting Scholar and Becas Iniciación Investigación. The financial support for EARLINET in the ACTRIS Research Infrastructure Project by the European Union's Horizon 2020 research and innovation program through project ACTRIS-2 (grant agreement No 654109) and ACTRIS-IMP (grant agreement No 871115). Tuukka Petäjä acknowledges funding through Academy of Finland Center of Excellence in Atmospheric Sciences and Academy of Finland projects (1307537, 337549) as well as European Commission via "Smart URBan Solutions for air quality, disasters and city growth", SMURBS and European Innovation Action "Healthy Outdoor Premises for Everyone", HOPE. The authors thankfully acknowledge the FEDER program for the instrumentation used in this work and the University of Granada that supported this study through the Excellence Units Program. Special thanks are given to Teresa Soriano and the staff of the Andalusian Institute of Agricultural and Fisheries Research and Training (IFAPA) for their support and kindness.

6 References

Alonso-Blanco, E., Gómez-Moreno, F.J., Artíñano, B., Iglesias-Samitier, S., Juncal-Bello, V., Piñeiro-Iglesias, M., López-Mahía, P., Pérez, N., Brines, M., Alastuey, A., García, M.I., Rodríguez, S., Sorribas, M., Águila, A. del, Titos, G., Lyamani, H., Alados-Arboledas, L., 2018. Temporal and spatial variability of atmospheric particle number size distributions across Spain. Atmos. Environ. 190, 146–160. https://doi.org/10.1016/j.atmosenv.2018.06.046

Alves, C., Vicente, A., Nunes, T., Gonçalves, C., Fernandes, A.P., Mirante, F., Tarelho, L., Sánchez de la Campa, A.M., Querol, X., Caseiro, A., Monteiro, C., Evtyugina, M., Pio, C., 2011. Summer

2009 wildfires in Portugal: Emission of trace gases and aerosol composition. Atmos. Environ. 45, 641–649. https://doi.org/10.1016/j.atmosenv.2010.10.031

Amato, F., Alastuey, A., Karanasiou, A., Lucarelli, F., Nava, S., Calzolai, G., Severi, M., Becagli, S., Gianelle, V.L., Colombi, C., Alves, C., Custódio, D., Nunes, T., Cerqueira, M., Pio, C., Eleftheriadis, K., Diapouli, E., Reche, C., Minguillón, M.C., Manousakas, M.I., Maggos, T., Vratolis, S., Harrison, R.M., Querol, X., 2016. AIRUSE-LIFE+: A harmonized PM speciation and source apportionment in five southern European cities. Atmos. Chem. Phys. 16, 3289–3309. https://doi.org/10.5194/acp-16-3289-2016

Andrews, E., Sheridan, P.J., Ogren, J.A., Hageman, D., Jefferson, A., Wendell, J., Alástuey, A., Alados-Arboledas, L., Bergin, M., Ealo, M., Gannet Hallar, A., Hoffer, A., Kalapov, I., Keywood, M., Kim, J., Kim, S.W., Kolonjari, F., Labuschagne, C., Lin, N.H., Macdonald, A., Mayol-Bracero, O.L., McCubbin, I.B., Pandolfi, M., Reisen, F., Sharma, S., Sheridan, J.P., Sorribas, M., Sun, J., 2019. Overview of the NOAA/ESRL federated aerosol network. Bull. Am. Meteorol. Soc. 100, 123–135. https://doi.org/10.1175/BAMS-D-17-0175.1

Beddows, D.C.S., Dall'Osto, M., Harrison, R.M., 2009. Cluster analysis of rural, urban, and curbside atmospheric particle size data. Environ. Sci. Technol. 43, 4694–4700. https://doi.org/10.1021/es803121t

Beddows, D.C.S., Harrison, R.M., Green, D.C., Fuller, G.W., 2015. Receptor modelling of both particle composition and size distribution from a background site in London, UK. Atmos. Chem. Phys. 15, 10107–10125. https://doi.org/10.5194/acp-15-10107-2015

Beelen, R., Hoek, G., van den Brandt, P.A., Goldbohm, R.A., Fischer, P., Schouten, L.J., Jerrett, M., Hughes, E., Armstrong, B., Brunekreef, B., 2008. Long-term effects of traffic-related air pollution on mortality in a Dutch cohort (NLCS-AIR study). Environ. Health Perspect. 116, 196–202. https://doi.org/10.1289/ehp.10767

Brauer, M., Hoek, G., Van Vliet, P., Meliefste, K., Fischer, P.H., Wijga, A., Koopman, L.P., Neijens, H.J., Gerritsen, J., Kerkhof, M., Heinrich, J., Bellander, T., Brunekreef, B., 2002. Air pollution from traffic and the development of respiratory infections and asthmatic and allergic symptoms in children. Am. J. Respir. Crit. Care Med. 166, 1092–1098. https://doi.org/10.1164/rccm.200108-007OC

Brines, M., Dall'Osto, M., Beddows, D.C.S., Harrison, R.M., Gómez-Moreno, F., Núñez, L., Artíñano, B., Costabile, F., Gobbi, G.P., Salimi, F., Morawska, L., Sioutas, C., Querol, X., 2015. Traffic and nucleation events as main sources of ultrafine particles in high-insolation developed world cities. Atmos. Chem. Phys. 15, 5929–5945. https://doi.org/10.5194/acp-15-5929-2015

Cai, J., Chu, B., Yao, L., Yan, C., Heikkinen, L. M., Zheng, F., Li, C., Fan, X., Zhang, S., Yang, D., Wang, Y., Kokkonen, T. V., Chan, T., Zhou, Y., Dada, L., Liu, Y., He, H., Paasonen, P., Kujansuu, J. T., Petäjä, T., Mohr, C., Kangasluoma, J., Bianchi, F., Sun, Y., Croteau, P. L., Worsnop, D. R., Kerminen, V.-M., Du, W., Kulmala, M., Daellenbach, K. R., 2020. Size-segregated particle number

and mass concentrations from different emission sources in urban Beijing, Atmos. Chem. Phys. 20, 12721–12740, https://doi.org/10.5194/acp-20-12721-2020

Casquero-Vera, J.A., Lyamani, H., Titos, G., Borrás, E., Olmo, F.J., Alados-Arboledas, L., 2019. Impact of primary NO2 emissions at different urban sites exceeding the European NO2 standard limit. Sci. Total Environ. 646, 1117–1125. https://doi.org/10.1016/j.scitotenv.2018.07.360

Casquero-Vera, J.A., Lyamani, H., Dada, L., Hakala, S., Paasonen, P., Román, R., Fraile, R., Petäjä, T., Olmo-Reyes, F.J., Alados-Arboledas, L., 2020. New particle formation at urban and high-altitude remote sites in the south-eastern Iberian Peninsula. Atmos. Chem. Phys. 20, 14253–14271. https://doi.org/10.5194/acp-20-14253-2020

Cassee, F., Morawska, L., Peters, A., Wierzbicka, A., Buonanno, G., Cyrys, J., SchnelleKreis, J., Kowalski, M., Riediker, M., Birmili, W., Querol, X., Yildirim, A.Ö., Elder, A., Yu, I.J., Øvrevik, J., Hougaard, K.S., Loft, S., Schmid, O., Schwarze, P.E., Stöger, T. Schneider, A., Okokon, E., Samoli, E., Stafoggia, M., Pickford, R., Zhang, S., Breitner, S., Schikowski, T., Lanki, T., Aurelio, T., 2019. White Paper: Ambient ultrafine particles evidence for policy makers. Thinking outside the box team. www.efca.net/files/WHITE%20PAPER-UFP%20evidence%20for%20policy%20makers%20(25%20OCT).pdf

Chan, T.W., Meloche, E., Kubsh, J., Brezny, R., 2014. Black carbon emissions in gasoline exhaust and a reduction alternative with a gasoline particulate filter. Environ. Sci. Technol. 48, 6027–6034. https://doi.org/10.1021/es501791b

Chen, T., Liu, Y., Ma, Q., Chu, B., Zhang, P., Liu, C., Liu, J., He, H., 2019. Significant source of secondary aerosol: Formation from gasoline evaporative emissions in the presence of SO2 and NH3. Atmos. Chem. Phys. 19, 8063–8081. https://doi.org/10.5194/acp-19-8063-2019

Costabile, F., Alas, H., Aufderheide, M., Avino, P., Amato, F., Argentini, S., Barnaba, F., Berico, M., Bernardoni, V., Biondi, R., Calzolai, G., Canepari, S., Casasanta, G., Ciampichetti, S., Conidi, A., Cordelli, E., Ianni, A. Di, Liberto, L. Di, Facchini, M.C., Facci, A., Frasca, D., Gilardoni, S., Grollino, M.G., Gualtieri, M., Lucarelli, F., Malaguti, A., Manigrasso, M., Montagnoli, M., Nava, S., Padoan, E., Perrino, C., Petralia, E., Petenko, I., Querol, X., Simonetti, G., Tranfo, G., Ubertini, S., Valli, G., Valentini, S., Vecchi, R., Volpi, F., Weinhold, K., Wiedensholer, A., Zanini, G., Gobbi, G.P., 2017. First results of the "Carbonaceous Aerosol in Rome and Environs (CARE)" Experiment: Beyond current standards for PM10. Atmosphere (Basel). 8. https://doi.org/10.3390/atmos8120249

Dal Maso, M., Kulmala, M., Riipinen, I., Wagner, R., Hussein, T., Aalto, P.P., Lehtinen, K.E.J., 2005. Formation and growth of fresh atmospheric aerosols: Eight years of aerosol size distribution data from SMEAR II, Hyytiälä, Finland. Boreal Environ. Res. 10, 323–336.

Del Águila, A., Sorribas, M., Lyamani, H., Titos, G., Olmo, F.J., Arruda-Moreira, G., Yela, M., Alados-Arboledas, L., 2018. Sources and physicochemical characteristics of submicron aerosols during

three intensive campaigns in Granada (Spain). Atmos. Res. 213, 398–410. https://doi.org/10.1016/j.atmosres.2018.06.004

Drinovec, L., Močnik, G., Zotter, P., Prévôt, A.S.H., Ruckstuhl, C., Coz, E., Rupakheti, M., Sciare, J., Müller, T., Wiedensohler, A., Hansen, A.D.A., 2015. The "dual-spot" Aethalometer: An improved measurement of aerosol black carbon with real-time loading compensation. Atmos. Meas. Tech. 8, 1965–1979. https://doi.org/10.5194/amt-8-1965-2015

Ealo, M., Alastuey, A., Ripoll, A., Pérez, N., Minguillón, M.C., Querol, X., Pandolfi, M., 2016. Detection of Saharan dust and biomass burning events using near-real-time intensive aerosol optical properties in the north-western Mediterranean. Atmos. Chem. Phys. 16, 12567–12586. https://doi.org/10.5194/acp-16-12567-2016

EEA, 2019. European Environment Agency. Air quality in Europe — 2019 report; https://www.eea.europa.eu/publications/air-quality-in-europe-2019

EMEP, 2016. Air pollution trends in the EMEP region between 1990 and 2012. Joint Report of the EMEP Task Force on Measurements and Modelling (TFMM), Chemical Co-ordinating Centre (CCC), Meteorological Synthesizing Centre-East (MSC-E), Meteorological Synthesizing Centre-West (MSC-W).
https://www.unece.org/fileadmin/DAM/env/documents/2016/AIR/Publications/Air_pollution_trends_in_the_EMEP_region.pdf

Favez, O., Cachier, H., Sciare, J., Sarda-Estève, R., Martinon, L., 2009. Evidence for a significant contribution of wood burning aerosols to PM2.5 during the winter season in Paris, France. Atmos. Environ. 43, 3640–3644. https://doi.org/10.1016/j.atmosenv.2009.04.035

Fernández-Camacho, R., Rodríguez, S., De La Rosa, J., Sánchez De La Campa, A.M., Viana, M., Alastuey, A., Querol, X., 2010. Ultrafine particle formation in the inland sea breeze airflow in Southwest Europe. Atmos. Chem. Phys. 10, 9615–9630. https://doi.org/10.5194/acp-10-9615-2010

Fuller, G.W., Tremper, A.H., Baker, T.D., Yttri, K.E., Butterfield, D., 2014. Contribution of wood burning to PM10 in London. Atmos. Environ. 87, 87–94. https://doi.org/10.1016/j.atmosenv.2013.12.037

Gómez-Moreno, F.J., Pujadas, M., Plaza, J., Rodríguez-Maroto, J.J., Martínez-Lozano, P., Artíñano, B., 2011. Influence of seasonal factors on the atmospheric particle number concentration and size distribution in Madrid. Atmos. Environ. 45, 3169–3180. https://doi.org/10.1016/j.atmosenv.2011.02.041

Hama, S.M.L., Cordell, R.L., Monks, P.S., 2017. Quantifying primary and secondary source contributions to ultrafine particles in the UK urban background. Atmos. Environ. 166, 62–78. https://doi.org/10.1016/j.atmosenv.2017.07.013

Hamilton, R.S., Mansfield, T.A., 1991. Airborne particulate elemental carbon: Its sources, transport and contribution to dark smoke and soiling. Atmos. Environ. Part A, Gen. Top. 25, 715–723. https://doi.org/10.1016/0960-1686(91)90070-N

Helin, A., Niemi, J. V., Virkkula, A., Pirjola, L., Teinilä, K., Backman, J., Aurela, M., Saarikoski, S., Rönkkö, T., Asmi, E., Timonen, H., 2018. Characteristics and source apportionment of black carbon in the Helsinki metropolitan area, Finland. Atmos. Environ. 190, 87–98. https://doi.org/10.1016/j.atmosenv.2018.07.022

Henschel, S., Querol, X., Atkinson, R., Pandolfi, M., Zeka, A., Le Tertre, A., Analitis, A., Katsouyanni, K., Chanel, O., Pascal, M., Bouland, C., Haluza, D., Medina, S., Goodman, P.G., 2013. Ambient air SO2 patterns in 6 European cities. Atmos. Environ. 79, 236–247. https://doi.org/10.1016/j.atmosenv.2013.06.008

Herich, H., Hueglin, C., Buchmann, B., 2011. A 2.5 year's source apportionment study of black carbon from wood burning and fossil fuel combustion at urban and rural sites in Switzerland. Atmos. Meas. Tech. 4, 1409–1420. https://doi.org/10.5194/amt-4-1409-2011

Hoek, G., Brunekreef, B., Verhoeff, A., V anWijnen, J., Fischer, P., 2000. Daily mortality and air pollution in the Netherlands. J. Air Waste Manag. Assoc. 50, 1380–1389. https://doi.org/10.1080/10473289.2000.10464182

Ito, K., Mathes, R., Ross, Z., Nádas, A., Thurston, G., Matte, T., 2011. Fine particulate matter constituents associated with cardiovascular hospitalizations and mortality in New York City. Environ. Health Perspect. 119, 467–473. https://doi.org/10.1289/ehp.1002667

Järvi, L., Rannik, Ü., Mammarella, I., Sogachev, A., Aalto, P.P., Keronen, P., Siivola, E., Kulmala, M., Vesala, T., 2009. Annual particle flux observations over a heterogeneous urban area. Atmos. Chem. Phys. 9, 7847–7856. https://doi.org/10.5194/acp-9-7847-2009

Johnston, C.J., Finkelstein, J.N., Mercer, P., Corson, N., Gelein, R., Oberdorster, G., 2000. Pulmonary effects induced by ultrafine PTFE particles. Toxicol. Appl. Pharmacol. 168, 208–215. https://doi.org/10.1006/taap.2000.9037

Kalogridis, A.C., Vratolis, S., Liakakou, E., Gerasopoulos, E., Mihalopoulos, N., Eleftheriadis, K., 2018. Assessment of wood burning versus fossil fuel contribution to wintertime black carbon and carbon monoxide concentrations in Athens, Greece. Atmos. Chem. Phys. 18, 10219–10236. https://doi.org/10.5194/acp-18-10219-2018

Karlsson, H.L., Gustafsson, J., Cronholm, P., Möller, L., 2009. Size-dependent toxicity of metal oxide particles-A comparison between nano- and micrometer size. Toxicol. Lett. 188, 112–118. https://doi.org/10.1016/j.toxlet.2009.03.014

Kerminen, V.M., Chen, X., Vakkari, V., Petäjä, T., Kulmala, M., Bianchi, F., 2018. Atmospheric new particle formation and growth: Review of field observations. Environ. Res. Lett. https://doi.org/10.1088/1748-9326/aadf3c

Kulmala, M., Luoma, K., Virkkula, A., Petäjä, T., Paasonen, P., Kerminen, V.M., Nie, W., Qi, X., Shen, Y., Chi, X., Ding, A., 2016. On the mode-segregated aerosol particle number concentration load: Contributions of primary and secondary particles in Hyytiälä and Nanjing. Boreal Environ. Res. 21, 319–331.

Laj, P., Bigi, A., Rose, C., Andrews, E., Lund Myhre, C., Collaud Coen, M., Lin, Y., Wiedensohler, A., Schulz, M., A. Ogren, J., Fiebig, M., Gliß, J., Mortier, A., Pandolfi, M., Petäja, T., Kim, S.W., Aas, W., Putaud, J.P., Mayol-Bracero, O., Keywood, M., Labrador, L., Aalto, P., Ahlberg, E., Alados Arboledas, L., Alastuey, A., Andrade, M., Artinano, B., Ausmeel, S., Arsov, T., Asmi, E., Backman, J., Baltensperger, U., Bastian, S., Bath, O., Paul Beukes, J., T. Brem, B., Bukowiecki, N., Conil, S., Couret, C., Day, D., Dayantolis, W., Degorska, A., Eleftheriadis, K., Fetfatzis, P., Favez, O., Flentje, H., I. Gini, M., Gregorič, A., Gysel-Beer, M., Gannet Hallar, A., Hand, J., Hoffer, A., Hueglin, C., K. Hooda, R., Hyvärinen, A., Kalapov, I., Kalivitis, N., Kasper-Giebl, A., Eun Kim, J., Kouvarakis, G., Kranjc, I., Krejci, R., Kulmala, M., Labuschagne, C., Lee, H.J., Lihavainen, H., Lin, N.H., Löschau, G., Luoma, K., Marinoni, A., Martins Dos Santos, S., Meinhardt, F., Merkel, M., Metzger, J.M., Mihalopoulos, N., Anh Nguyen, N., Ondracek, J., Pérez, N., Rita Perrone, M., Pichon, J.M., Picard, D., Pichon, J.M., Pont, V., Prats, N., Prenni, A., Reisen, F., Romano, S., Sellegri, K., Sharma, S., Schauer, G., Sheridan, P., Patrick Sherman, J., Schütze, M., Schwerin, A., Sohmer, R., Sorribas, M., Steinbacher, M., Sun, J., Titos, G., Toczko, B., Tuch, T., Tulet, P., Tunved, P., Vakkari, V., Velarde, F., Velasquez, P., Villani, P., Vratolis, S., Wang, S.H., Weinhold, K., Weller, R., Yela, M., Yus-Diez, J., Zdimal, V., Zieger, P., Zikova, N., 2020. A global analysis of climate-relevant aerosol properties retrieved from the network of Global Atmosphere Watch (GAW) near-surface observatories. Atmos. Meas. Tech. 13, 4353–4392. https://doi.org/10.5194/amt-13-4353-2020

Liakakou, E., Stavroulas, I., Kaskaoutis, D.G., Grivas, G., Paraskevopoulou, D., Dumka, U.C., Tsagkaraki, M., Bougiatioti, A., Oikonomou, K., Sciare, J., Gerasopoulos, E., Mihalopoulos, N., 2020. Long-term variability, source apportionment and spectral properties of black carbon at an urban background site in Athens, Greece. Atmos. Environ. 222, 117137. https://doi.org/10.1016/j.atmosenv.2019.117137

Lyamani, H., Olmo, F.J., Alados-Arboledas, L., 2010. Physical and optical properties of aerosols over an urban location in Spain: Seasonal and diurnal variability. Atmos. Chem. Phys. 10, 239–254. https://doi.org/10.5194/acp-10-239-2010

Lyamani, H., Olmo, F.J., Foyo, I., Alados-Arboledas, L., 2011. Black carbon aerosols over an urban area in south-eastern Spain: Changes detected after the 2008 economic crisis. Atmos. Environ. 45, 6423–6432. https://doi.org/10.1016/j.atmosenv.2011.07.063

Lyamani, H., Casquero-Vera, J.A., Titos, G., Moreira, G. de A., Benavent-Oltra, J.A., Conte, M., Contini, D., Järvi, L., Olmo-Reyes, F.J. and Alados-ArboledasL., 2020. Aerosol number fluxes and concentrations over a southern European urban area, Manuscript submitted for publication.

Merikanto, J., Spracklen, D. V., Mann, G.W., Pickering, S.J., Carslaw, K.S., 2009. Impact of nucleation on global CCN. Atmos. Chem. Phys. 9, 8601–8616. https://doi.org/10.5194/acp-9-8601-2009

Minguillón, M.C., Ripoll, A., Pérez, N., Prévôt, A.S.H., Canonaco, F., Querol, X., Alastuey, A., 2015. Chemical characterization of submicron regional background aerosols in the western Mediterranean using an Aerosol Chemical Speciation Monitor. Atmos. Chem. Phys. 15, 6379–6391. https://doi.org/10.5194/acp-15-6379-2015

Moreira, G. de A., Guerrero-Rascado, J.L., Bravo-Aranda, J.A., Foyo-Moreno, I., Cazorla, A., Alados, I., Lyamani, H., Landulfo, E., Alados-Arboledas, L., 2020. Study of the planetary boundary layer height in an urban environment using a combination of microwave radiometer and ceilometer. Atmos. Res. 240. https://doi.org/10.1016/j.atmosres.2020.104932

Murray, C. J. L., Aravkin, A. Y., Zheng, P., Abbafati, C., Abbas, K. M., Abbasi-Kangevari, M., Abd-Allah, F., Abdelalim, A., Abdollahi, M., Abdollahpour, I., Abegaz, K. H., Abolhassani, H., Aboyans, V., Abreu, L. G., Abrigo, M. R. M., Abualhasan, A., Abu-Raddad, L. J., Abushouk, A. I., Adabi, M., Adekanmbi, V., Adeoye, A. M., Adetokunboh, O. O., Adham, D., Advani, S. M., Agarwal, G., Aghamir, S. M. K., Agrawal, A., Ahmad, T., Ahmadi, K., Ahmadi, M., Ahmadieh, H., Ahmed, M. B., Akalu, T. Y., Akinyemi, R. O., Akinyemiju, T., Akombi, B., Akunna, C. J., Alahdab, F., Al-Aly, Z., Alam, K., Alam, S., Alam, T., Alanezi, F. M., Alanzi, T. M., Alemu, B. wassihun, Alhabib, K. F., Ali, M., Ali, S., Alicandro, G., Alinia, C., Alipour, V., Alizade, H., Aljunid, S. M., Alla, F., Allebeck, P., Almasi-Hashiani, A., Al-Mekhlafi, H. M., Alonso, J., Altirkawi, K. A., Amini-Rarani, M., Amiri, F., Amugsi, D. A., Ancuceanu, R., Anderlini, D., Anderson, J. A., Andrei, C. L., Andrei, T., Angus, C., Anjomshoa, M., Ansari, F., Ansari-Moghaddam, A., Antonazzo, I. C., Antonio, C. A. T., Antony, C. M., Antriyandarti, E., Anvari, D., Anwer, R., Appiah, S. C. Y., Arabloo, J., Arab-Zozani, M., Ariani, F., Armoon, B., Ärnlöv, J., Arzani, A., Asadi-Aliabadi, M., Asadi-Pooya, A. A., Ashbaugh, C., Assmus, M., Atafar, Z., Atnafu, D. D., Atout, M. M. W., Ausloos, F., Ausloos, M., Ayala Quintanilla, B. P., Ayano, G., Ayanore, M. A., Azari, S., Azarian, G., Azene, Z. N., et al. , 2020. Global burden of 87 risk factors in 204 countries and territories, 1990–2019: a systematic analysis for the Global Burden of Disease Study 2019, Lancet, 396(10258), 1223–1249, doi:10.1016/S0140-6736(20)30752-2.

Nam, E., Kishan, S., Baldauf, R.W., Fulper, C.R., Sabisch, M., Warila, J., 2010. Temperature effects on particulate matter emissions from light-duty, gasoline-powered motor vehicles. Environ. Sci. Technol. 44, 4672–4677. https://doi.org/10.1021/es100219q

Németh, Z., Rosati, B., Zíková, N., Salma, I., Bozó, L., Dameto de España, C., Schwarz, J., Ždímal, V., Wonaschütz, A., 2018. Comparison of atmospheric new particle formation events in three Central European cities. Atmos. Environ. 178, 191–197. https://doi.org/10.1016/j.atmosenv.2018.01.035

Ng, N.L., Herndon, S.C., Trimborn, A., Canagaratna, M.R., Croteau, P.L., Onasch, T.B., Sueper, D., Worsnop, D.R., Zhang, Q., Sun, Y.L., Jayne, J.T., 2011. An Aerosol Chemical Speciation

Monitor (ACSM) for routine monitoring of the composition and mass concentrations of ambient aerosol. Aerosol Sci. Technol. 45, 780–794. https://doi.org/10.1080/02786826.2011.560211

Nieminen, T., Kerminen, V.M., Petäjä, T., Aalto, P.P., Arshinov, M., Asmi, E., Baltensperger, U., Beddows, D.C.S., Paul Beukes, J., Collins, D., Ding, A., Harrison, R.M., Henzing, B., Hooda, R., Hu, M., Hõrrak, U., Kivekäs, N., Komsaare, K., Krejci, R., Kristensson, A., Laakso, L., Laaksonen, A., Richard Leaitch, W., Lihavainen, H., Mihalopoulos, N., Németh, Z., Nie, W., O'Dowd, C., Salma, I., Sellegri, K., Svenningsson, B., Swietlicki, E., Tunved, P., Ulevicius, V., Vakkari, V., Vana, M., Wiedensohler, A., Wu, Z., Virtanen, A., Kulmala, M., 2018. Global analysis of continental boundary layer new particle formation based on long-term measurements. Atmos. Chem. Phys. 18, 14737–14756. https://doi.org/10.5194/acp-18-14737-2018

Olivares, G., Johansson, C., Ström, J., Hansson, H.C., 2007. The role of ambient temperature for particle number concentrations in a street canyon. Atmos. Environ. 41, 2145–2155. https://doi.org/10.1016/j.atmosenv.2006.10.068

Ortiz-Amezcua, P., 2019. Atmospheric profiling based on Aerosol and Doppler lidar., [online] Available from: http://hdl.handle.net/10481/57771 (Accessed 15 June 2020).

Ostro, B., Feng, W.Y., Broadwin, R., Green, S., Lipsett, M., 2007. The effects of components of fine particulate air pollution on mortality in California: Results from CALFINE. Environ. Health Perspect. 115, 13–19. https://doi.org/10.1289/ehp.9281

Pakkanen, T.A., Kerminen, V.M., Ojanen, C.H., Hillamo, R.E., Aarnio, P., Koskentalo, T., 2000. Atmospheric black carbon in Helsinki. Atmos. Environ. 34, 1497–1506. https://doi.org/10.1016/S1352-2310(99)00344-1

Pandolfi, M., Alados-Arboledas, L., Alastuey, A., Andrade, M., Angelov, C., Artiñano, B., Backman, J., Baltensperger, U., Bonasoni, P., Bukowiecki, N., Collaud Coen, M., Conil, S., Coz, E., Crenn, V., Dudoitis, V., Ealo, M., Eleftheriadis, K., Favez, O., Fetfatzis, P., Fiebig, M., Flentje, H., Ginot, P., Gysel, M., Henzing, B., Hoffer, A., Holubova Smejkalova, A., Kalapov, I., Kalivitis, N., Kouvarakis, G., Kristensson, A., Kulmala, M., Lihavainen, H., Lunder, C., Luoma, K., Lyamani, H., Marinoni, A., Mihalopoulos, N., Moerman, M., Nicolas, J., O'Dowd, C., Petäjä, T., Petit, J.E., Marc Pichon, J., Prokopciuk, N., Putaud, J.P., Rodríguez, S., Sciare, J., Sellegri, K., Swietlicki, E., Titos, G., Tuch, T., Tunved, P., Ulevicius, V., Vaishya, A., Vana, M., Virkkula, A., Vratolis, S., Weingartner, E., Wiedensohler, A., Laj, P., 2018. A European aerosol phenomenology - 6: Scattering properties of atmospheric aerosol particles from 28 ACTRIS sites. Atmos. Chem. Phys. 18, 7877–7911. https://doi.org/10.5194/acp-18-7877-2018

Patrón, D., Lyamani, H., Titos, G., Casquero-Vera, J.A., Cardell, C., Močnik, G., Alados-Arboledas, L., Olmo, F.J., 2017. Monumental heritage exposure to urban black carbon pollution. Atmos. Environ. 170, 22–32. https://doi.org/10.1016/j.atmosenv.2017.09.030

Putaud, J.P., Van Dingenen, R., Alastuey, A., Bauer, H., Birmili, W., Cyrys, J., Flentje, H., Fuzzi, S., Gehrig, R., Hansson, H.C., Harrison, R.M., Herrmann, H., Hitzenberger, R., Hüglin, C., Jones,

A.M., Kasper-Giebl, A., Kiss, G., Kousa, A., Kuhlbusch, T.A.J., Löschau, G., Maenhaut, W., Molnar, A., Moreno, T., Pekkanen, J., Perrino, C., Pitz, M., Puxbaum, H., Querol, X., Rodriguez, S., Salma, I., Schwarz, J., Smolik, J., Schneider, J., Spindler, G., ten Brink, H., Tursic, J., Viana, M., Wiedensohler, A., Raes, F., 2010. A European aerosol phenomenology - 3: Physical and chemical characteristics of particulate matter from 60 rural, urban, and kerbside sites across Europe. Atmos. Environ. 44, 1308–1320. https://doi.org/10.1016/j.atmosenv.2009.12.011

Querol, X., Alastuey, A., Pandolfi, M., Reche, C., Pérez, N., Minguillón, M.C., Moreno, T., Viana, M., Escudero, M., Orio, A., Pallarés, M., Reina, F., 2014. 2001-2012 trends on air quality in Spain. Sci. Total Environ. 490, 957–969. https://doi.org/10.1016/j.scitotenv.2014.05.074

Reche, C., Querol, X., Alastuey, A., Viana, M., Pey, J., Moreno, T., Rodríguez, S., González, Y., Fernández-Camacho, R., De La Campa, A.M.S., De La Rosa, J., Dall'Osto, M., Prévôt, A.S.H., Hueglin, C., Harrison, R.M., Quincey, P., 2011. New considerations for PM, Black Carbon and particle number concentration for air quality monitoring across different European cities. Atmos. Chem. Phys. 11, 6207–6227. https://doi.org/10.5194/acp-11-6207-2011

Ripamonti, G., Järvi, L., Mølgaard, B., Hussein, T., Nordbo, A., Hämeri, K., 2013. The effect of local sources on aerosol particle number size distribution, concentrations and fluxes in Helsinki, Finland. Tellus, Ser. B Chem. Phys. Meteorol. 65. https://doi.org/10.3402/tellusb.v65i0.19786

Rodríguez, S., Cuevas, E., 2007. The contributions of "minimum primary emissions" and "new particle formation enhancements" to the particle number concentration in urban air. J. Aerosol Sci. 38, 1207–1219. https://doi.org/10.1016/j.jaerosci.2007.09.001

Rönkkö, T., Kuuluvainen, H., Karjalainen, P., Keskinen, J., Hillamo, R., Niemi, J. V., Pirjola, L., Timonen, H.J., Saarikoski, S., Saukko, E., Järvinen, A., Silvennoinen, H., Rostedt, A., Olin, M., Yli-Ojanperä, J., Nousiainen, P., Kousa, A., Dal Maso, M., 2017. Traffic is a major source of atmospheric nanocluster aerosol. Proc. Natl. Acad. Sci. U. S. A. 114, 7549–7554. https://doi.org/10.1073/pnas.1700830114

Salma, I., Borsós, T., Weidinger, T., Aalto, P., Kulmala, M., 2014. Comparative study of ultrafine atmospheric aerosol within a city. Atmos. Environ. 92, 154–161. https://doi.org/10.1016/j.atmosenv.2014.04.020

Sandradewi, J., Prévôt, A.S.H., Szidat, S., Perron, N., Alfarra, M.R., Lanz, V.A., Weingartner, E., Baltensperger, U.R.S., 2008. Using aerosol light abosrption measurements for the quantitative determination of wood burning and traffic emission contribution to particulate matter. Environ. Sci. Technol. 42, 3316–3323. https://doi.org/10.1021/es702253m

Singh, V., Ravindra, K., Sahu, L., Sokhi, R., 2018. Trends of atmospheric black carbon concentration over United Kingdom. Atmos. Environ. 178, 148–157. https://doi.org/10.1016/j.atmosenv.2018.01.030

Sorribas, M., Adame, J.A., Olmo, F.J., Vilaplana, J.M., Gil-Ojeda, M., Alados-Arboledas, L., 2015. A long-term study of new particle formation in a coastal environment: Meteorology, gas phase and solar radiation implications. Sci. Total Environ. 511, 723–737. https://doi.org/10.1016/j.scitotenv.2014.12.011

Tao, J., Zhang, L., Cao, J., Zhang, R., 2017. A review of current knowledge concerning PM2. 5 chemical composition, aerosol optical properties and their relationships across China. Atmos. Chem. Phys. https://doi.org/10.5194/acp-17-9485-2017

Titos, G., del Águila, A., Cazorla, A., Lyamani, H., Casquero-Vera, J.A., Colombi, C., Cuccia, E., Gianelle, V., Močnik, G., Alastuey, A., Olmo, F.J., Alados-Arboledas, L., 2017. Spatial and temporal variability of carbonaceous aerosols: Assessing the impact of biomass burning in the urban environment. Sci. Total Environ. 578, 613–625. https://doi.org/10.1016/j.scitotenv.2016.11.007

Titos, G., Lyamani, H., Pandolfi, M., Alastuey, A., Alados-Arboledas, L., 2014. Identification of fine (PM1) and coarse (PM10-1) sources of particulate matter in an urban environment. Atmos. Environ. 89, 593–602. https://doi.org/10.1016/j.atmosenv.2014.03.001

Wang, F., Cernuschi, S., Ozgen, S., Ripamonti, G., Vecchi, R., Valli, G., Lonati, G., 2016. UFP and BC at a mid-sized city in Po valley, Italy: Size resolved partitioning between primary and newly formed particles. Atmos. Environ. 142, 120–131. https://doi.org/10.1016/j.atmosenv.2016.07.030

WHO, 2013. Review of Evidence on Health Aspects on Air Pollution e REVIHAAP Project. Technical Report. WHO Regional Office for Europe, Copenhagen, Denmark. http://www.euro.who.int/__data/assets/pdf_file/0004/193108/REVIHAAP-Final-technical-report.pdf.

Wiedensohler, A., Wiesner, A., Weinhold, K., Birmili, W., Hermann, M., Merkel, M., Müller, T., Pfeifer, S., Schmidt, A., Tuch, T., Velarde, F., Quincey, P., Seeger, S., Nowak, A., 2018. Mobility particle size spectrometers: Calibration procedures and measurement uncertainties. Aerosol Sci. Technol. 52, 146–164. https://doi.org/10.1080/02786826.2017.1387229

Credit Author Statement

JACV: Conceptualization, Investigation, Methodology, Data curation, Formal analysis, Writing - original draft, Visualization. **HL:** Conceptualization, Investigation, Methodology, Supervision, Writing - review & editing. **GT:** Investigation, Writing - review & editing. **MCM:** Writing - review & editing. **LD:** Writing - review & editing. **AA:** Writing - review & editing. **XQ:** Writing - review & editing. **TP:** Writing - review & editing. **FJO:** Supervision, Project administration, Writing - review & editing, Funding acquisition. **LAA:** Supervision, Project administration, Writing - review & editing, Funding acquisition.

Declaration of competing interest

The authors declare that they have no known competing financial interests or personal relationships that could have appeared to influence the work reported in this paper.

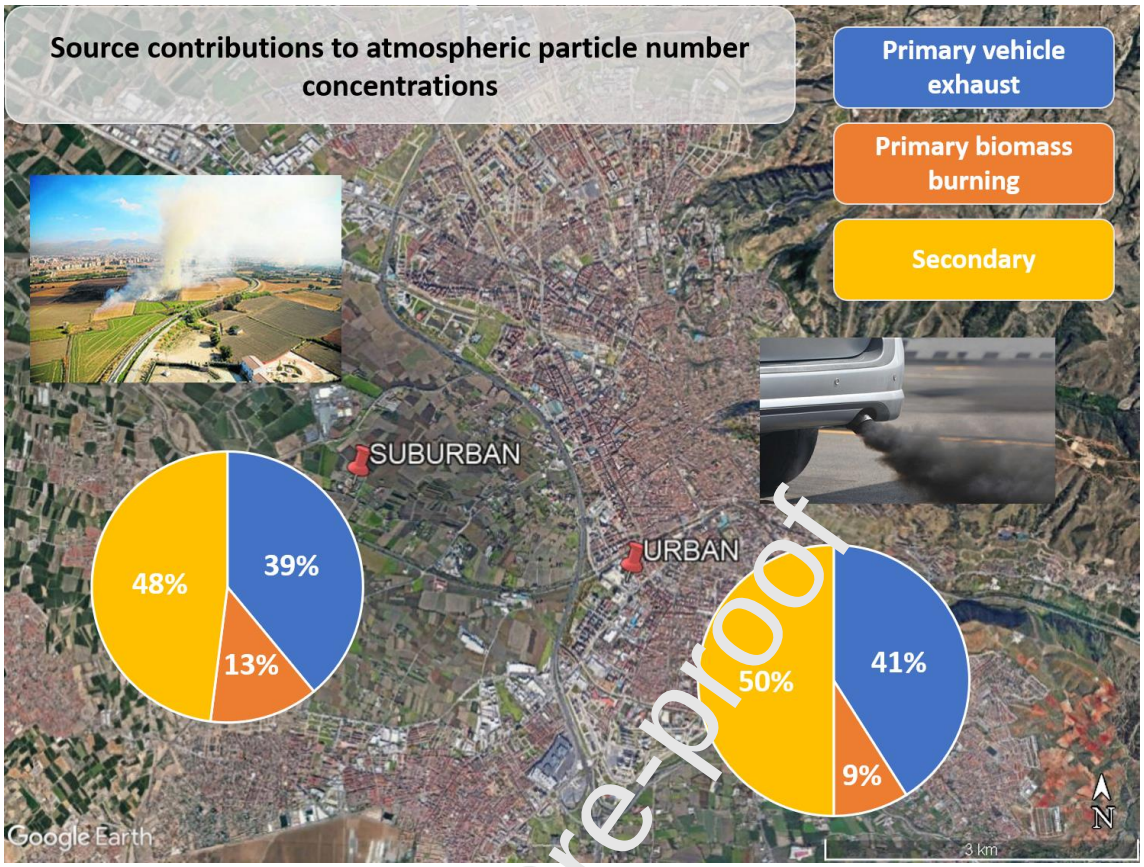

Graphical abstract

Highlights:

- New method to estimate contributions of primary and secondary particles is proposed
- Traffic primary emissions contribute up to 65% at high urban aerosol load
- Size-segregated particles from traffic and biomass burning sources are investigated
- Biomass burning emissions significantly contribute to primary particles
- New particle formation is an important source of particles during summer noon hours